Onset and decay of the 1+1 Hawking-Unruh effect: what the derivative-coupling detector saw

Benito A. Juárez-Aubry[*] and Jorma Louko[†]

School of Mathematical Sciences
University of Nottingham
Nottingham NG7 2RD
UK

Abstract

We study an Unruh-DeWitt particle detector that is coupled to the proper time derivative of a real scalar field in 1+1 spacetime dimensions. Working within first-order perturbation theory, we cast the transition probability into a regulator-free form, and we show that the transition rate remains well defined in the limit of sharp switching. The detector is insensitive to the infrared ambiguity when the field becomes massless, and we verify explicitly the regularity of the massless limit for a static detector in Minkowski half-space. We then consider a massless field for two scenarios of interest for the Hawking-Unruh effect: an inertial detector in Minkowski spacetime with an exponentially receding mirror, and an inertial detector in $(1 + 1)$-dimensional Schwarzschild spacetime, in the Hartle-Hawking-Israel and Unruh vacua. In the mirror spacetime the transition rate traces the onset of an energy flux from the mirror, with the expected Planckian late time asymptotics. In the Schwarzschild spacetime the transition rate of a detector that falls in from infinity gradually loses thermality, diverging near the singularity proportionally to $r^{-3/2}$.

---

[*]pmxbaju@nottingham.ac.uk

[†]jorma.louko@nottingham.ac.uk

arXiv:1406.2574v3 [gr-qc] 25 Nov 2014

1 Introduction

For quantum fields living on a pseudo-Riemannian manifold, the experiences of observers coupled to the field depend both on the quantum state of the field and on the worldline of the observer [1, 2]. A celebrated example is the Unruh effect [3], in which uniformly accelerated observers in Minkowski spacetime experience a thermal bath in the quantum state that inertial observers perceive as void of particles. Other well-studied examples arise with black holes that emit Hawking radiation [4] and with observers in spacetimes of high symmetry [5].

A useful tool for analysing the experiences of an observer is a model particle detector that follows the observer's worldline and has internal states that couple to the quantum field. Such detectors are known as Unruh-DeWitt (UDW) detectors [3, 6]. While much of the early literature on the UDW detectors focused on stationary situations, including the Unruh effect [7, 8], the detectors remain well defined also in time-dependent situations, where they can be analysed within first-order perturbation theory [9, 10, 11, 12, 13, 14, 15, 16, 17, 18, 19, 20, 21] as well as by nonperturbative techniques [22, 23, 24, 25, 26]. A review with further references can be found in [27].

In this paper we consider a detector coupled to a quantised scalar field in 1+1 spacetime dimensions. A scalar field in 1+1 dimensions has local propagating degrees of freedom, and it exhibits the Hawking and Unruh effects just like a scalar field in higher dimensions. However, the dynamics of the field in 1+1 dimensions is significantly simpler than in higher dimensions, especially for a massless minimally coupled field, for which the field equation is conformally invariant and conformal techniques are available. In particular, the evolution of a massles minimally coupled field on a (1+1)-dimensional collapsing star spacetime reduces essentially to that of a massless field on (1+1)-dimensional Minkowski spacetime in the presence of a receding mirror, and the system is explicitly solvable [28, 29].

The simplifications in the dynamics in $1 + 1$ dimensions come however at a cost: the Wightman function of a minimally coupled field in 1+1 dimensions is infrared divergent in the massless limit. While Hadamard states can still can be defined in terms of the short distance expansion of the Wightman function [30], the Hadamard expansion contains an additive constant that is not determined by the quantum state. While this undetermined additive constant does not contribute to stress-energy expectation values [1, 31, 32], it does contribute to the transition probability of an UDW detector that couples to the value of the field at the detector's location. In stationary situations the ambiguous contribution to transition probablities can be argued to vanish, under suitable assumptions about the switch-on and switch-off [7, 11, 12], but in nonstationary situations the ambiguity is more severe and has been found to lead to physically undesirable predictions in examples that include a receding mirror spacetime [19].

In this paper we analyse a detector that is insensitive to the infrared ambiguity of the $(1 + 1)$-dimensional Wightman function in the massless minimaly coupled limit: we couple the detector linearly to the *derivative* of the field with respect to the detector's proper time [9, 22, 33, 34], rather than to the value of the field. Working in first-

order perturbation theory, the detector's transition probability involves then the double derivative of the Wightman function, rather than the Wightman function itself. We show that the response of the $(1+1)$-dimensional derivative-coupling detector is closely similar to that of the $(3+1)$-dimensional detector with a non-derivative coupling [14, 15]. In particular, the transition probablity can be written as an integral formula that involves no short-distance regulator at the coincidence limit but contains instead an additive term that depends only on the switching function that controls the switch-on and switch-off. A consequence is that in the limit of sharp switching the transition probability diverges but the transition rate remains finite.

We carry out three checks on the physical reasonableness of the derivative-coupling detector in stationary situations in which the switch-on is pushed to asymptotically early times. First, we verify that the transition rate is continuous in the limit of vanishing mass for an inertial detector in Minkowski space, with the field in Minkowski vacuum, and we show that the same holds also for a static detector in Minkowski half-space with Dirichlet and Neumann boundary conditions. This is evidence that the derivative coupling manages to remove the infrared ambiguity of the massless field without producing unexpected discontinuities in the massless limit. Second, we show that the transition rate of a uniformly accelerated detector in Minkowski space, coupled to a massless field in Minkowski vacuum, coincides with that of an inertial detector at rest with a thermal bath, being in particular thermal in the sense of the Kubo-Martin-Schwinger (KMS) property [35, 36]. This shows that the derivative-coupling detector sees the usual Unruh effect for a massless field. Third, we show that in a thermal bath of a massless field in Minkowski space, the transition rate of an inertial detector that is moving with respect to the bath is a sum of two terms that are individually thermal but at different temperatures, related to the temperature of the bath by Doppler shifts to the red and to the blue. As these terms stem respectively from the right-moving and left-moving components of the field, the temperature shifts are exactly as one would expect.

After these checks, we focus on the massless minimally coupled field in two nonstationary situations, each of interest for the Hawking-Unruh effect.

We first consider a Minkowski spacetime with a mirror whose exponentially receding motion makes the field mimic the late time behaviour of a field in a collapsing star spacetime [1, 28, 29]. We show that at late times the detector's transition rate is the sum of a Planckian contribution, corresponding to the field modes propagating away from the mirror, and a vacuum contribution, corresponding to the field modes propagating towards the mirror. While the detector couples to the sum of the two parts, the two parts can nevertheless be unambiguously identified by considering their dependence on the detector's velocity with respect to the rest frame in which the mirror was static in the asymptotic past. We also show numerical results on how the transition rate evolves from the asymptotic early time form to the asymptotic late time form. These properties of the transition rate are in full agreement with the energy flux emitted by the mirror [1, 28, 29].

We then consider a detector falling inertially into the $(1 + 1)$-dimensional Schwarz-

schild black hole, with the field in the Hartle-Hawking-Israel (HHI) and Unruh vacua. Starting the infall at the asymptotic infinity, we verify that the early time transition rate in the HHI vacuum is as in a thermal state, in the usual Hawking temperature, while in the Unruh vacuum it is as in a thermal state for the outgoing field modes and in the Boulware vacuum for the ingoing field modes. The outgoing and ingoing contributions can again be unambiguously identified by considering their dependence on the detector's velocity in the asymptotic past. The transition rate remains manifestly nonsingular on horizon-crossing, and we present numerical evidence of how the thermal properties are gradually lost during the infall. Near the black hole singularity the transition rate diverges proportionally to $r^{-3/2}$ where r is the Schwarzschild radial coordinate. These results are in full agreement with the known properties of the HHI and Unruh vacua, including their thermality, their invariance under Schwarzschild time translations and their regularity across the future horizon.

We anticipate that the derivative-coupling detector will be a useful tool for probing a quantum field in other situations where the infrared properties raise technical difficulties for the conventional UDW detector. One such instance is when the field has zero modes, which typically occur in spacetimes with compact spatial sections [37]. Other instances may arise in analogue spacetime systems [38] or in spacetimes where the back-reaction due to Hawking evaporation is strong (for a small selection of references see [39, 40, 41, 42, 43]).

The structure of the paper is as follows. In Section 2 we introduce the derivative-coupling detector, write the transition probability in a regulator-free form and provide the formula for the transition rate in the sharp switching limit. Consistency checks in three stationary situations are carried out in Section 3. Sections 4 and 5 address respectively the receding mirror spacetime and the Schwarzschild spacetime. The results are summarised and discussed in Section 6. Details of technical calculations are deferred to four appendices.

Our metric signature is $(-+)$, so that the norm squared of a timelike vector is negative. We use units in which $c = \hbar = k_B = 1$, so that frequencies, energies and temperatures have dimension inverse length. Spacetime points are denoted by Sans Serif characters (x) and spacetime indices are denoted by $a, b, \ldots$. Complex conjugation is denoted by overline. $O(x)$ denotes a quantity for which $O(x)/x$ is bounded as $x \to 0$, $o(x)$ denotes a quantity for which $o(x)/x \to 0$ as $x \to 0$, $O(1)$ denotes a quantity that is bounded in the limit under consideration, and $o(1)$ denotes a quantity that goes to zero in the limit under consideration.

2   Derivative-coupling detector

In this section we introduce an UDW detector that couples linearly to the proper time derivative of a scalar field [9, 22, 33, 34]. We show, within first-order perturbation theory, that in $(1 + 1)$ spacetime dimensions the detector's transition probability and transition rate are closely similar to those of a $(3 + 1)$-dimensional UDW detector with

a non-derivative coupling [14, 15].

2.1   Derivative-coupling detector in $d \geq 2$ dimensions

Our detector is a spatially point-like quantum system with two distinct energy eigenstates. We denote the normalised energy eigenstates by $|0\rangle_D$ and $|\omega\rangle_D$, with the respective energy eigenvalues 0 and ω, where $\omega \neq 0$.

The detector moves in a spacetime of dimension $d \geq 2$ along the smooth timelike worldline $\mathsf{x}(\tau)$, where τ is the proper time, and it couples to a real scalar field ϕ via the interaction Hamiltonian

$$H_{\text{int}} = c\chi(\tau)\mu(\tau)\frac{d}{d\tau}\phi\big(\mathsf{x}(\tau)\big) \ , \tag{2.1}$$

where c is a coupling constant, μ is the detector's monopole moment operator and the switching function χ specifies how the interaction is switched on an off. We assume that χ is real-valued, non-negative and smooth with compact support.

Where H_{int} (2.1) differs from the usual UDW detector [3, 6] is that the interaction is linear in the proper time derivative of the field, rather than in the field itself. An alternative expression is $H_{\text{int}} = c\chi(\tau)\mu(\tau)\dot{\mathsf{x}}^a\nabla_a\phi\big(\mathsf{x}(\tau)\big)$, where the overdot denotes $d/d\tau$.

We take the detector to be initially in the state $|0\rangle_D$ and the field to be in a state $|\psi\rangle$, which we assume to be regular in the sense of the Hadamard property [30]. After the interaction has been turned on and off, we are interested in the probability for the detector to have made a transition to the state $|\omega\rangle_D$, regardless the final state of the field. Working in first-order perturbation theory in c, we may adapt the analysis of the usual UDW detector [1, 2] to show that this probability factorises as

$$P(\omega) = c^2|{}_D\langle 0|\mu(0)|\omega\rangle_D|^2\mathcal{F}(\omega) \ , \tag{2.2}$$

where $|{}_D\langle 0|\mu(0)|\omega\rangle_D|^2$ depends only on the internal structure of the detector but neither on $|\psi\rangle$, the trajectory or the switching, while the dependence on $|\psi\rangle$, the trajectory and the switching is encoded in the response function $\mathcal{F}$. With our H_{int} (2.1), the response function is given by

$$\mathcal{F}(\omega) = \int_{-\infty}^{\infty} d\tau' \int_{-\infty}^{\infty} d\tau'' \, \mathrm{e}^{-\mathrm{i}\omega(\tau'-\tau'')} \, \chi(\tau')\chi(\tau'') \, \partial_{\tau'}\partial_{\tau''}\mathcal{W}(\tau', \tau'') \ , \tag{2.3}$$

where the correlation function $\mathcal{W}(\tau', \tau'') \doteq \langle\psi|\phi\big(\mathsf{x}(\tau')\big)\phi\big(\mathsf{x}(\tau'')\big)|\psi\rangle$ is the pull-back of the Wightman function $\langle\psi|\phi(\mathsf{x}')\phi(\mathsf{x}'')|\psi\rangle$ to the detector's world line.

From now on we drop the constant prefactors in (2.2) and refer to the response function as the transition probability.

As $|\psi\rangle$ is Hadamard and the detector's worldline is smooth and timelike, the correlation function $\mathcal{W}$ is a well-defined distribution on $\mathbb{R} \times \mathbb{R}$ [44, 45, 46, 47]. As χ is smooth with compact support, it follows that $\mathcal{F}$ (2.3) is well defined: given a family of functions $\mathcal{W}_\epsilon$ that converges to the distribution $\mathcal{W}$ as $\epsilon \to 0_+$, $\mathcal{F}$ is evaluated by first

making in (2.3) the replacement $\mathcal{W} \to \mathcal{W}_\epsilon$, then performing the integrals, and finally taking the limit $\epsilon \to 0_+$. The limit $\epsilon \to 0_+$ may however not necessarily be taken under the integrals. For the usual UDW detector, for which the response function is given as in (2.3) but without the derivatives, this issue is known to become subtle if one wishes to define an instantaneous transition rate by passing to the limit of sharp switching: the subtleties start in three spacetime dimensions and increase as the spacetime dimension increases and the correlation function becomes more singular at the coincidence limit [14, 15, 16, 17]. We may expect similar subtleties for the derivative-coupling detector, and since the derivatives in (2.3) increase the singularity of the integrand at the coincidence limit, we may expect the subtleties to start in lower spacetime dimensions than for the usual UDW detector.

We confirm these expectations in subsections 2.2, 2.3 and 2.4 by analysing the response function (2.3) and the transition rate in $(1+1)$ spacetime dimensions.

2.2 $(1+1)$ response function: isolating the coincidence limit

We now specialise to $(1 + 1)$ spacetime dimensions. In this subsection we write the response function (2.3) in a way where the contribution from the singularity of the integrand at the coincidence limit has been isolated.

We start from (2.3) and write $\mathcal{W} = (\mathcal{W} - \mathcal{W}_{\text{sing}}) + \mathcal{W}_{\text{sing}}$, where $\mathcal{W}_{\text{sing}}$ is the locally integrable function

$$
\mathcal{W}_{\text{sing}}(\tau', \tau'') \doteq \begin{cases} -\dfrac{\mathrm{i}\,\mathrm{sgn}(\tau' - \tau'')}{4} - \dfrac{\ln|\tau' - \tau''|}{2\pi} & \text{for } \tau' \neq \tau'', \\ 0 & \text{for } \tau' = \tau'', \end{cases} \tag{2.4}
$$

and sgn denotes the signum function,

$$
\mathrm{sgn}\, x \doteq \begin{cases} 1 & \text{for } x > 0, \\ 0 & \text{for } x = 0, \\ -1 & \text{for } x < 0. \end{cases} \tag{2.5}
$$

We obtain

$$
\mathcal{F}(\omega) = \mathcal{F}_{\text{reg}}(\omega) + \mathcal{F}_{\text{sing}}(\omega), \tag{2.6a}
$$

$$
\mathcal{F}_{\text{reg}}(\omega) = \int_{-\infty}^{\infty} d\tau' \int_{-\infty}^{\infty} d\tau'' \, \mathrm{e}^{-\mathrm{i}\omega(\tau'-\tau'')} \chi(\tau')\chi(\tau'') \, \partial_{\tau'}\partial_{\tau''} \big[\mathcal{W}(\tau', \tau'') - \mathcal{W}_{\text{sing}}(\tau', \tau'')\big], \tag{2.6b}
$$

$$
\mathcal{F}_{\text{sing}}(\omega) = \int_{-\infty}^{\infty} d\tau' \int_{-\infty}^{\infty} d\tau'' \, \mathrm{e}^{-\mathrm{i}\omega(\tau'-\tau'')} \chi(\tau')\chi(\tau'') \, \partial_{\tau'}\partial_{\tau''} \mathcal{W}_{\text{sing}}(\tau', \tau''), \tag{2.6c}
$$

where the derivatives are understood in the distributional sense.

Consider first $\mathcal{F}_{\text{reg}}$ (2.6b). The Hadamard short distance form of the Wightman function [30] implies that both $\mathcal{W}(\tau', \tau'')$ and $\partial_{\tau'}\partial_{\tau''}[\mathcal{W}(\tau', \tau'') - \mathcal{W}_{\text{sing}}(\tau', \tau'')]$ are represented in a neighbourhood of $\tau' = \tau''$ by locally integrable functions. It follows that the integral in (2.6b) receives no distributional contributions from $\tau' = \tau''$, and the integral can hence be decomposed into integrals over the subdomains $\tau' > \tau''$ and $\tau' < \tau''$. In the subdomain $\tau' > \tau''$ we write $\tau' = u$ and $\tau'' = u - s$, where $u \in \mathbb{R}$ and $0 < s < \infty$, and in the subdomain $\tau' < \tau''$ we write $\tau'' = u$ and $\tau' = u - s$, where again $u \in \mathbb{R}$ and $0 < s < \infty$. Using the property $\mathcal{W}(\tau', \tau'') = \overline{\mathcal{W}(\tau'', \tau')}$ and the explicit form of $\mathcal{W}_{\text{sing}}(\tau', \tau'')$ (2.4), we obtain

$$\mathcal{F}_{\text{reg}}(\omega) = 2 \int_{-\infty}^{\infty} du \int_{0}^{\infty} ds \, \chi(u)\chi(u-s) \operatorname{Re}\left[e^{-i\omega s}\left(\mathcal{A}(u, u-s) + \frac{1}{2\pi s^2}\right)\right], \qquad (2.7)$$

where

$$\mathcal{A}(\tau', \tau'') \doteq \partial_{\tau'}\partial_{\tau''}\mathcal{W}(\tau', \tau''). \qquad (2.8)$$

Note that the integrand in (2.7) is still a distribution, but it is represented by a locally integrable function in a neighbourhood of $s = 0$, and any distributional singularities are hence isolated from $s = 0$.

We evaluate $\mathcal{F}_{\text{sing}}$ (2.6c) in Appendix A. Combining (2.7) and (A.6), we find

$$\mathcal{F}(\omega) = -\omega\Theta(-\omega)\int_{-\infty}^{\infty} du\,[\chi(u)]^2 + \frac{1}{\pi}\int_{0}^{\infty} ds\,\frac{\cos(\omega s)}{s^2}\int_{-\infty}^{\infty} du\,\chi(u)[\chi(u) - \chi(u-s)]$$

$$+ 2\int_{-\infty}^{\infty} du \int_{0}^{\infty} ds\,\chi(u)\chi(u-s)\operatorname{Re}\left[e^{-i\omega s}\left(\mathcal{A}(u, u-s) + \frac{1}{2\pi s^2}\right)\right], \qquad (2.9)$$

where $\mathcal{A}$ is given by (2.8) and Θ is the Heaviside function,

$$\Theta(x) \doteq \begin{cases} 1 & \text{for } x > 0, \\ 0 & \text{for } x \le 0. \end{cases} \qquad (2.10)$$

An equivalent form, using for $\mathcal{F}_{\text{sing}}$ the alternative expression (A.7) given in Appendix A, is

$$\mathcal{F}(\omega) = -\frac{\omega}{2}\int_{-\infty}^{\infty} du\,[\chi(u)]^2 + \frac{1}{\pi}\int_{0}^{\infty}\frac{ds}{s^2}\int_{-\infty}^{\infty} du\,\chi(u)\,[\chi(u) - \chi(u-s)]$$

$$+ 2\int_{-\infty}^{\infty} du \int_{0}^{\infty} ds\,\chi(u)\chi(u-s)\operatorname{Re}\left[e^{-i\omega s}\mathcal{A}(u, u-s) + \frac{1}{2\pi s^2}\right]. \qquad (2.11)$$

The integral over s in the second term in (2.9) and (2.11) is convergent at small s since the integral over u produces an even function of s that vanishes at $s = 0$.

The expression (2.11) for the response function is closely similar to that obtained in [14, 15] for the usual, non-derivative UDW detector in $(3 + 1)$ dimensions. This

happens because of the similarity between the coincidence limit singularities of the twice differentiated $(1 + 1)$-dimensional correlation function, appearing in (2.3), and the undifferentiated $(3 + 1)$-dimensional correlation function that appears in the similar expression for non-derivative coupling.

We re-emphasise that the last term in (2.9) and (2.11) may contain distributional contributions from $s > 0$. Similar distributional contributions were not considered for the $(3 + 1)$-dimensional non-derivative UDW detector in [15], but they can occur also there, and the analysis in [15] can be amended to include these contributions by proceeding as in the present paper. Similar distributional contributions can arise in any spacetime dimension: in $(2 + 1)$ dimensions, examples on the Bañdados-Teitelboim-Zanelli black hole were encountered in [17].

2.3 $(1 + 1)$ sharp switching limit: transition rate

In this subsection we consider the sharp switching limit of the derivative-coupling detector in $(1 + 1)$ dimensions.

Following [14, 15], we consider a family of switching functions given by

$$\chi(u) = h_1\left(\frac{u - \tau_0 + \delta}{\delta}\right) \times h_2\left(\frac{-u + \tau + \delta}{\delta}\right), \tag{2.12}$$

where τ and τ_0 are pararameters satisfying $\tau > \tau_0$, δ is a positive parameter, and h_1 and h_2 are smooth non-negative functions such that $h_1(x) = h_2(x) = 0$ for $x \leq 0$ and $h_1(x) = h_2(x) = 1$ for $x \geq 1$. In words, the detector is switched on over an interval of duration δ before time τ_0, stays on at constant coupling from time τ_0 to time τ, and is finally switched off over an interval of duration δ after time τ. The profile of the switch-on is determined by h_1 and the profile of the switch-off is determined by h_2.

We are interested in the limit $\delta \to 0$. To begin with, suppose that $\mathcal{A}(\tau', \tau'')$ (2.8) is represented by a smooth function for $\tau' \neq \tau''$. Given the similarity between (2.11) and the $(3 + 1)$-dimensional non-derivative response function given by equation (3.16) in [15], we may follow the analysis that led to equations (4.4) and (4.5) in [15]. For the response function, we find

$$\mathcal{F}(\omega, \tau) = -\frac{\omega \Delta\tau}{2} + 2 \int_{\tau_0}^{\tau} du \int_0^{u - \tau_0} ds \, \text{Re}\left[e^{-i\omega s}\mathcal{A}(u, u - s) + \frac{1}{2\pi s^2}\right]$$

$$+ \frac{1}{\pi}\ln\left(\frac{\Delta\tau}{\delta}\right) + C + O(\delta), \tag{2.13}$$

where $\Delta\tau \doteq \tau - \tau_0$, C is a constant that depends only on h_1 and h_2, and we have included in $\mathcal{F}(\omega, \tau)$ the second argument τ to indicate explicitly the dependence on τ.

The response function (2.13) hence diverges logarithmically as $\delta \to 0$, but the divergent contribution is a pure switching effect, independent of the quantum state and of

the detector's trajectory. The transition rate, defined as $\dot{\mathcal{F}}(\omega,\tau) \doteq \frac{\partial}{\partial \tau}\mathcal{F}(\omega,\tau)$, remains finite as $\delta \to 0$, and is in this limit given by

$$\dot{\mathcal{F}}(\omega,\tau) = -\frac{\omega}{2} + 2\int_0^{\Delta\tau} ds\, \mathrm{Re}\left[\mathrm{e}^{-\mathrm{i}\omega s}\mathcal{A}(\tau,\tau-s) + \frac{1}{2\pi s^2}\right] + \frac{1}{\pi\Delta\tau}\;. \qquad (2.14)$$

An equivalent expression, obtained by writing $1 = \cos(\omega s) + [1 - \cos(\omega s)]$ under the integral in (2.14), is

$$\dot{\mathcal{F}}(\omega,\tau) = -\omega\Theta(-\omega) + \frac{1}{\pi}\left[\frac{\cos(\omega\Delta\tau)}{\Delta\tau} + |\omega|\,\mathrm{si}(|\omega|\Delta\tau)\right]$$

$$+ 2\int_0^{\Delta\tau} ds\, \mathrm{Re}\left[\mathrm{e}^{-\mathrm{i}\omega s}\left(\mathcal{A}(\tau,\tau-s) + \frac{1}{2\pi s^2}\right)\right]\;, \qquad (2.15)$$

where si is the sine integral in the notation of [48]. When the switch-on is in the asymptotic past and the fall-off of $\mathcal{A}(\tau,\tau-s)$ is sufficiently fast as large s, the $\Delta\tau \to \infty$ limit of (2.15) gives

$$\dot{\mathcal{F}}(\omega,\tau) = -\omega\Theta(-\omega) + 2\int_0^{\infty} ds\, \mathrm{Re}\left[\mathrm{e}^{-\mathrm{i}\omega s}\left(\mathcal{A}(\tau,\tau-s) + \frac{1}{2\pi s^2}\right)\right]\;. \qquad (2.16)$$

The observational meaning of the transition rate relates to ensembles of ensembles of detectors (see Section 5.3.1 of [12] or Section 2 of [15]).

When $\mathcal{A}(\tau',\tau'')$ (2.8) is not represented by a smooth function for $\tau' \neq \tau''$, the estimates leading to (2.13) and (2.14) need not hold, and the transition rate need not have a well-defined $\delta \to 0$ limit for all τ_0 and τ. In particular, if the detector is switched on at a finite time τ_0 and $\mathcal{A}(\tau',\tau'')$ has a distributional singularity at $(\tau',\tau'') = (\tau,\tau_0)$, the integral expressions in (2.14) and (2.15) would not be well defined because the singularity occurs at an end-point of the integration. If the switch-on is in the asymptotic past, however, the transition rate formula (2.16) is well defined even when $\mathcal{A}(\tau',\tau'')$ has distributional singularities for $\tau' \neq \tau''$ provided these singularities are sufficiently isolated. We shall encounter examples of such singularities in subsection 3.1 and Section 4.

Similar remarks about singularities of the correlation function at timelike-separated points apply also to the sharp switching limit of the non-derivative UDW detector in $(3+1)$ dimensions. The transition rate results given in [15] for a switch-on at a finite time hold when no such singularities are present.

2.4 Stationary transition rate

Suppose that the Wightman function is stationary with respect to the detector's trajectory, in the sense that $\mathcal{W}(\tau',\tau'')$ depends on τ' and τ'' only through the difference $\tau' - \tau''$. When the detector is switched on in the asymptotic past, the transition rate

(2.16) reduces to

$$\dot{\mathcal{F}}(\omega) = -\omega\Theta(-\omega) + 2\int_0^\infty ds\,\mathrm{Re}\left[\mathrm{e}^{-\mathrm{i}\omega s}\left(\mathcal{A}(s,0) + \frac{1}{2\pi s^2}\right)\right]$$

$$= -\omega\Theta(-\omega) + \int_{-\infty}^\infty ds\,\mathrm{e}^{-\mathrm{i}\omega s}\left[\mathcal{A}(s,0) + \frac{1}{2\pi s^2}\right]$$

$$= -\omega\Theta(-\omega) + \int_C ds\,\mathrm{e}^{-\mathrm{i}\omega s}\left[\mathcal{A}(s,0) + \frac{1}{2\pi s^2}\right]$$

$$= \int_{-\infty}^\infty ds\,\mathrm{e}^{-\mathrm{i}\omega s}\,\mathcal{A}(s,0)\ , \tag{2.17}$$

where we have dropped the second argument τ from $\dot{\mathcal{F}}$ as the transition rate is now independent of τ, and $\mathcal{A}(s,0)$ is understood as a distribution everywhere, including $s = 0$. In (2.17) we have first used the properties $\mathcal{A}(\tau',\tau'') = \mathcal{A}(\tau'-\tau'',0)$ and $\mathcal{A}(\tau',\tau'') = \overline{\mathcal{A}(\tau'',\tau')}$. Next, we have deformed the real s axis into a contour C in the complex s plane, such that C follows the real axis except that it dips into the lower half-plane near $s = 0$; this deformation is justified by the Hadamard short separation form of the Wightman function [30]. In the contour integral over C, we have then separated the two terms in the integrand, evaluated the integral of the second term by a standard contour technique, and noted that in the first term C can be deformed back to the real s axis provided the integrand is understood as a distribution for all s, including $s = 0$.

The result (2.17) coincides with the transition rate that one obtains from the response function (2.3) by the usual procedure of setting $\chi = 1$ and formally factoring out the infinite total detection time [1].

3   Stationary checks: massless limit, the Unruh effect, and inertial response in a thermal bath

In this section we perform reasonableness checks on the derivative-coupling detector in three stationary situations. First, we verify that the transition rate is continuous in the massless limit for a static detector in Minkowski space, and also in Minkowski half-space with Dirichlet and Neumann boundary conditions. Second, we verify that the detector sees the usual Unruh effect when the field is massless. Third, we verify that the transition rate of an inertial detector in the thermal bath of a massless field sees a Doppler shift when the detector has a nonvanishing velocity in the inertial frame of the bath.

3.1   Static detector in Minkowski (half-)space

Let $\mathcal{M}$ be $(1+1)$ Minkowski spacetime, with standard Minkowski coordinates (t, x) in which the metric reads $ds^2 = -dt^2 + dx^2$, and let $\widetilde{\mathcal{M}}$ be the submanifold of $\mathcal{M}$ in which

$x > 0$. We consider in $\mathcal{M}$ and $\widetilde{\mathcal{M}}$ a scalar field of mass $m \geq 0$, and in $\widetilde{\mathcal{M}}$ we impose the Dirichlet or Neumann boundary condition that the field or its normal derivative vanish at $x = 0$.

We set the field in $\mathcal{M}$ in the Minkowski vacuum $|0\rangle$, and the field in $\widetilde{\mathcal{M}}$ in the Minkowski-like vacuum $|\tilde{0}\rangle$ that is the no-particle state with respect to the timelike Killing vector ∂_t.

Now, consider in $\mathcal{M}$ and $\widetilde{\mathcal{M}}$ a detector on the static worldline

$$\mathsf{x}(\tau) = (\tau, d) \ , \tag{3.1}$$

where d is a positive constant. In $\mathcal{M}$ the value of d has no geometric significance, but in $\widetilde{\mathcal{M}}$ d is the distance of the detector from the mirror at $x = 0$. We take the detector to be switched on in the asymptotic past, so that the detector's transition rate is stationary and given by (2.17). We shall show that the transition rate is continuous in the limit $m \to 0$.

3.1.1 $m > 0$

For $m > 0$, the Wightman function in $\mathcal{M}$ is [1]

$$\langle 0|\phi(\mathsf{x})\phi(\mathsf{x}')|0\rangle = \frac{1}{2\pi} K_0 \left[m\sqrt{(\Delta x)^2 - (\Delta t - \mathrm{i}\epsilon)^2} \right] \ , \tag{3.2}$$

where $\Delta x = x - x'$, $\Delta t = t - t'$, K_0 is the modified Bessel function of the second kind [48], and the expression is understood as a distribution in the sense of $\epsilon \to 0_+$. The square root is positive when x and x' are spacelike separated and $\epsilon \to 0_+$, and the continuation to general x and x' is specified by the $\mathrm{i}\epsilon$ prescription. By the method of images, the Wightman function in $\widetilde{\mathcal{M}}$ is the sum of (3.2) and the image piece

$$\langle \tilde{0}|\phi(\mathsf{x})\phi(\mathsf{x}')|\tilde{0}\rangle - \langle 0|\phi(\mathsf{x})\phi(\mathsf{x}')|0\rangle = \frac{\eta}{2\pi} K_0 \left[m\sqrt{(x + x')^2 - (\Delta t - \mathrm{i}\epsilon)^2} \right] \ , \tag{3.3}$$

where $\eta = -1$ for Dirichlet and $\eta = 1$ for Neumann.

We evaluate the transition rate (2.17) in Appendix B. We obtain

$$\mathcal{M}: \qquad \dot{\mathcal{F}}(\omega) = \frac{\omega^2}{\sqrt{\omega^2 - m^2}} \Theta(-\omega - m) \ , \tag{3.4a}$$

$$\widetilde{\mathcal{M}}: \qquad \dot{\mathcal{F}}(\omega) = \frac{\omega^2 \left[1 + \eta \cos\left(2d\sqrt{\omega^2 - m^2} \right) \right]}{\sqrt{\omega^2 - m^2}} \Theta(-\omega - m) \ . \tag{3.4b}$$

The transition rate is non-negative, and it is nonvanishing only for $\omega < -m$, that is, for de-excitations exceeding the mass gap. These are properties that one would expect of a reasonable detector coupled to a massive field.

3.1.2 $m = 0$

On $\mathcal{M}$, the massive Wightman function (3.2) diverges as $m \to 0$. However, the quantity $\langle 0|\phi(\mathsf{x})\phi(\mathsf{x}')|0\rangle + \frac{1}{2\pi}\ln[me^{\gamma}/(2\mu)]$, where γ is Euler's constant and μ is a positive constant of dimension inverse length, has at $m \to 0$ a finite limit, given by [48]

$$\langle 0|\phi(\mathsf{x})\phi(\mathsf{x}')|0\rangle \doteq -\frac{1}{2\pi}\ln\left[\mu\sqrt{(\Delta x)^2 - (\Delta t - \mathrm{i}\epsilon)^2}\right] . \tag{3.5}$$

We take (3.5) as the definition of the Wightman function for $m = 0$. The constant μ is required for dimensional consistency, and its arbitrariness means that $\langle 0|\phi(\mathsf{x})\phi(\mathsf{x}')|0\rangle$ (3.5) is unique up to an additive constant. The massless Wightman function on $\widetilde{\mathcal{M}}$ is the sum of (3.5) and the image piece

$$\langle \tilde{0}|\phi(\mathsf{x})\phi(\mathsf{x}')|\tilde{0}\rangle - \langle 0|\phi(\mathsf{x})\phi(\mathsf{x}')|0\rangle = -\frac{\eta}{2\pi}\ln\left[\mu\sqrt{(x + x')^2 - (\Delta t - \mathrm{i}\epsilon)^2}\right] , \tag{3.6}$$

where again $\eta = -1$ for Dirichlet and $\eta = 1$ for Neumann. Note that for $\eta = -1$, the massless Wightman function on $\widetilde{\mathcal{M}}$ is independent of μ and can be obtained as the $m \to 0$ limit of the massive Wightman function on $\widetilde{\mathcal{M}}$ without introducing a subtraction by hand.

We show in Appendix B that the transition rate is given by

$$\mathcal{M}: \qquad \dot{\mathcal{F}}(\omega) = -\omega\,\Theta(-\omega) , \tag{3.7a}$$

$$\widetilde{\mathcal{M}}: \qquad \dot{\mathcal{F}}(\omega) = -\omega\left[1 + \eta\cos(2d\omega)\right]\Theta(-\omega) . \tag{3.7b}$$

The transition rate is non-negative, and it is nonvanishing only for de-excitations, as one would expect of a reasonable detector coupled to a massless field.

We see from (3.4) and (3.7) that the massless transition rate is equal to the massless limit of the massive transition rate. This is the property that we wished to verify.

3.2   Unruh effect

Let again $\mathcal{M}$ be $(1 + 1)$ Minkowski spacetime, and consider in $\mathcal{M}$ a massless field in the Minkowski vacuum. We consider a detector on the uniformly accelerated worldline

$$\mathsf{x}(\tau) = \left(a^{-1}\sinh(a\tau), a^{-1}\cosh(a\tau)\right) , \tag{3.8}$$

where the positive constant a is the magnitude of the proper acceleration. The trajectory is stationary with respect to the boost Killing vector $t\partial_x + x\partial_t$, and $|0\rangle$ is invariant under this Killing vector. With the detector switch-on pushed to the asymptotic past, the transition rate is independent of time and given by (2.17).

From (2.8), (3.5) and (3.8), we find

$$\mathcal{A}(\tau', \tau'') = -\frac{a^2}{8\pi\sinh^2\left(a(\tau' - \tau'' - \mathrm{i}\epsilon)/2\right)} . \tag{3.9}$$

Substituting (3.9) in (2.17), deforming the contour of s-integration to $s = -i\pi/a + r$ where $r \in \mathbb{R}$, and using formula 3.985.1 in [49], we find

$$\dot{\mathcal{F}}(\omega) = \frac{\omega}{e^{2\pi\omega/a} - 1} \; . \tag{3.10}$$

The transition rate (3.10) satisfies the KMS relation [35, 36],

$$\dot{\mathcal{F}}(\omega) = e^{-\omega/T} \dot{\mathcal{F}}(-\omega) \; , \tag{3.11}$$

with $T = a/(2\pi)$, and is hence thermal at temperature $a/(2\pi)$ in the KMS sense. We conclude that the detector does see the usual Unruh effect [3, 7]. The Planckian form of the transition rate (3.10) is identical to that of a non-derivative detector coupled to a massless field on a uniformly accelerated trajectory in $(3 + 1)$ dimensions [3, 7].

3.3 Inertial detector in a thermal bath

We consider again a massless field in $(1 + 1)$ Minkowski spacetime $\mathcal{M}$, but now in the thermal state $|T\rangle$ of positive temperature T. Working in Minkowski coordinates (t, x) in which the thermal bath is at rest, the thermal Wightman function is obtained from the vacuum Wightman function by taking an image sum in t with period i/T [1]. With the vacuum Wightman function (3.5), the sum reads

$$\langle T|\phi(\mathsf{x})\phi(\mathsf{x}')|T\rangle = -\frac{1}{4\pi} \sum_{n=-\infty}^{\infty} \ln\left\{\mu^2 \left[(\Delta x)^2 - (\Delta t - i\epsilon + in/T)^2\right]\right\} \; , \tag{3.12}$$

and does not converge. However, differentiation of the sum in (3.12) term by term with respect to Δx gives a new sum that converges and can be summed by residues into an elementary function. We integrate the elementary function with respect to Δx and fix the Δt-dependent integration constant by requiring that the massless Klein-Gordon equation is satisfied, and requiring evenness in Δt for $(\Delta x)^2 - (\Delta t)^2 > 0$. The outcome is

$$\langle T|\phi(\mathsf{x})\phi(\mathsf{x}')|T\rangle \doteq -\frac{1}{4\pi} \ln\{\sinh[\pi T(\Delta x + \Delta t - i\epsilon)]\}$$
$$-\frac{1}{4\pi} \ln\{\sinh[\pi T(\Delta x - \Delta t + i\epsilon)]\} \; , \tag{3.13}$$

uniquely up to an additive constant, and we take (3.13) as the definition of the thermal Wightman function. Note that (3.13) decomposes into the right-mover contribution that depends on $\Delta(x - t)$ and the left-mover contribution that depends on $\Delta(x + t)$.

We consider the inertial detector worldline

$$\mathsf{x}(\tau) = (\tau \cosh\lambda, -\tau \sinh\lambda) \; , \tag{3.14}$$

13

where $\lambda \in \mathbb{R}$ is the detector's rapidity parameter with respect to the rest frame of the bath. For later convenience, we have chosen the sign in (3.14) so that a detector with positive λ is moving towards decreasing x. From (2.8), (3.13) and (3.14) we find

$$\mathcal{A}(\tau', \tau'') = -\frac{1}{16\pi} \left(\frac{(2\pi T_+)^2}{\sinh^2[\pi T_+(\tau' - \tau'' - i\epsilon)]} + \frac{(2\pi T_-)^2}{\sinh^2[\pi T_-(\tau' - \tau'' - i\epsilon)]} \right) , \quad (3.15)$$

where $T_\pm \doteq e^{\pm\lambda}T$. Taking the detector to be switched on in the asymptotic past, and proceeding as with (3.9), we find that the transition rate is given by

$$\dot{\mathcal{F}}(\omega) = \frac{\omega}{2} \left(\frac{1}{e^{\omega/T_+} - 1} + \frac{1}{e^{\omega/T_-} - 1} \right) , \quad (3.16)$$

simplifying in the special case $\lambda = 0$ to

$$\dot{\mathcal{F}}(\omega) = \frac{\omega}{e^{\omega/T} - 1} . \quad (3.17)$$

The $\lambda = 0$ transition rate (3.17) satisfies the KMS relation (3.11) in temperature T, and it coincides with the transition rate (3.10) of a uniformly accelerated detector when $T = a/(2\pi)$. The $\lambda \neq 0$ transition rate (3.16) is a sum of the right-mover and left-mover contributions, each satisfying the KMS relation but in the respective Doppler-shifted temperatures $T_\pm$. These are properties that one would expect of a reasonable detector.

3.4 Inertial detector with vacuum left-movers and thermal right-movers

In preparation for the nonstationary situations that will be addressed in Sections 4 and 5, we consider here the inertial detector (3.14) in the state in which the left-movers are in the Minkowski vacuum but the right-movers are in a thermal bath with temperature T. As the left-movers and the right-movers decouple, the results can be read off from those given above in a straightforward way. Taking the switch-on to the asymptotic past, we find

$$\dot{\mathcal{F}}(\omega) = -\frac{\omega}{2}\Theta(-\omega) + \frac{\omega}{2\left(e^{\omega/T_+} - 1\right)} . \quad (3.18)$$

The first term in (3.18) is the left-mover contribution, equal to half of the Minkowski transition rate. The second term is the right-mover contribution, which is Planckian in the Doppler-shifted temperature $T_+ = e^\lambda T$.

4 The receding mirror spacetime

In this section we consider a massless field in $(1+1)$-dimensional Minkowski spacetime with a receding mirror that asymptotes at late times to a null line, in a fashion that

14

mimics the late time redshift that occurs in a collapsing star spacetime [1, 28, 29]. Focusing on a specific mirror trajectory that is asymptotically inertial at early times, and choosing a vacuum with no incoming radiation from infinity, we compute the transition rate of an inertial, sharply-switched detector that is turned on in the asymptotic past. We show that the early time transition rate is Minkowskian and the late time transition rate has the expected form of Planckian radiation emitted from the mirror.

4.1 Mirror spacetime and the in-vacuum

Denoting a standard set of Minkowski coordinates by (t, x), we work in the double null coordinates

$$u = t - x \ , \tag{4.1a}$$

$$v = t + x \ , \tag{4.1b}$$

in which $ds^2 = -du\,dv$. We take the mirror trajectory to be

$$v = -\frac{1}{\kappa}\ln(1 + e^{-\kappa u}) \ , \tag{4.2}$$

where κ is a positive constant. When parametrised in terms of the proper time τ, the trajectory reads

$$u = -\frac{2}{\kappa}\ln[\sinh(-\kappa\tau/2)] \ , \tag{4.3a}$$

$$v = -\frac{2}{\kappa}\ln[\cosh(-\kappa\tau/2)] \ , \tag{4.3b}$$

where $-\infty < \tau < 0$. The velocity and acceleration are towards decreasing x, and the proper acceleration has the magnitude $\kappa/\sinh(-\kappa\tau)$. At early times the trajectory is asymptotically inertial, asymptoting to $x = 0$ from the left, with proper acceleration that vanishes exponentially in τ. At late times the trajectory asymptotes to the null line $v = 0$ from below, receding to infinity as $\tau \to 0_-$, and the proper acceleration diverges as $-1/\tau$. A spacetime diagram is shown in Figure 1.

We consider the spacetime that is to the right of the mirror. The mirror is hence receding, and the constant κ is analogous to the surface gravity in a collapsing star spacetime at late times [1, 28, 29].

We consider a massless scalar field ϕ with Dirichlet boundary conditions at the mirror. As the positive frequency mode functions, we choose [1, 28, 29]

$$u_k = i(4\pi k)^{-1/2}\left[e^{-ikv} - e^{-ikp(u)}\right] \ , \tag{4.4}$$

where $k > 0$ and

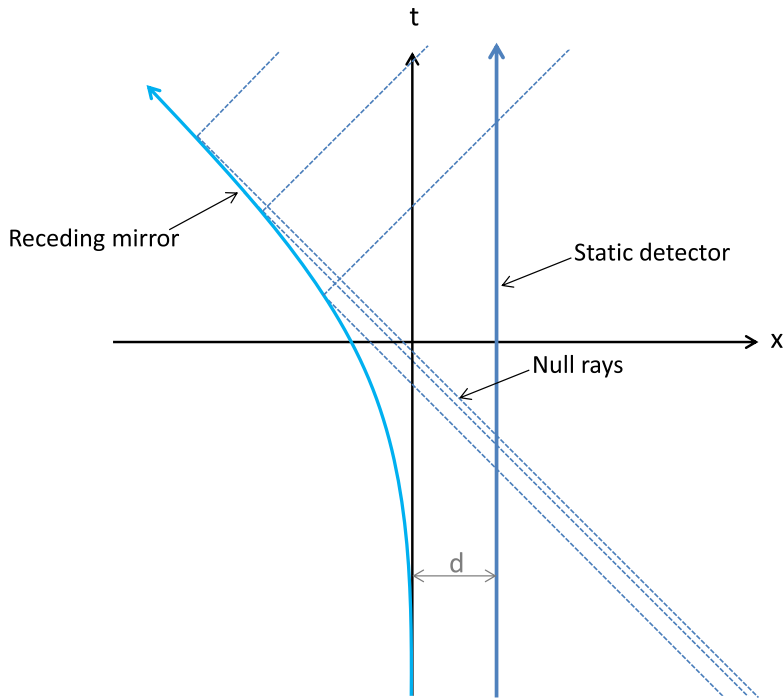$$p(u) = -\frac{1}{\kappa}\ln(1 + e^{-\kappa u}) \ . \tag{4.5}$$

15

Figure 1: Minkowski spacetime with the receding mirror (4.2) and an inertial detector (3.1) that is static with respect to the mirror in the asymptotic past. Dashed lines show a selection of null geodesics that bounce off the mirror.

These modes satisfy the massless Klein-Gordon equation, they satisfy the Dirichlet boundary condition at the mirror, and they are Dirac orthormal, $(u_k, u_{k'}) = -(\overline{u_k}, \overline{u_{k'}}) = \delta(k - k')$ and $(\overline{u_k}, u_{k'}) = (u_k, \overline{u_{k'}}) = 0$, where $(\cdot, \cdot)$ is the Klein-Gordon inner product on a hypersurface of constant t. In the distant past, the modes reduce to the usual Dirichlet boundary condition modes in the static half-space $x > 0$. We note that to verify the orthonormality, it suffices to consider the static half-space limit on a constant t hypersurface in the distant past: the inner product is constant in t due to the Klein-Gordon equation and the Dirichlet boundary condition.

We denote by $|0, \text{in}\rangle$ the no-particle state with respect to the modes (4.4). In the distant past, $|0, \text{in}\rangle$ coincides with the usual no-particle state in the half-space $x > 0$, and we call it the in-vacuum. Computing the Wightman as a mode sum from (4.4)

16

gives [1]

$$\langle 0, \text{in}|\phi(\mathsf{x})\phi(\mathsf{x}')|0, \text{in}\rangle = -\frac{1}{4\pi} \ln\left[\frac{\big(p(u) - p(u') - \text{i}\epsilon\big)(v - v' - \text{i}\epsilon)}{\big(v - p(u') - \text{i}\epsilon\big)\big(p(u) - v' - \text{i}\epsilon\big)}\right] , \tag{4.6}$$

where $\text{i}\epsilon$ arises from the conditional ultraviolet convergence as usual. The mode sum is infrared convergent because of the Dirichlet boundary condition.

4.2 Inertial detector: static in the distant past

We consider a detector on the inertial worldline (3.1), where d is again a positive constant. In the asymptotic past, the detector is hence at distance d from a static mirror. We take the detector to be switched on in the asymptotic past, and we take the field to be in the in-vacuum $|0, \text{in}\rangle$.

Using (3.1), (4.1) and (4.6), we find

$$\mathcal{A}(\tau', \tau'') = -\frac{1}{4\pi}\left(\frac{p'(u')p'(u'')}{[p(u') - p(u'') - \text{i}\epsilon]^2} + \frac{1}{(v' - v'' - \text{i}\epsilon)^2}\right.$$

$$\left. - \frac{p'(u'')}{[v' - p(u'') - \text{i}\epsilon]^2} - \frac{p'(u')}{[p(u') - v'' - \text{i}\epsilon]^2}\right) , \tag{4.7}$$

where $u' = \tau' - d$, $v' = \tau' + d$, $u'' = \tau'' - d$ and $v'' = \tau'' + d$. The prime on p denotes derivative with respect to the argument. From (2.16) we then have

$$\dot{\mathcal{F}}(\omega, \tau) = \dot{\mathcal{F}}_0(\omega, \tau) + \dot{\mathcal{F}}_1(\omega, \tau) + \dot{\mathcal{F}}_2(\omega, \tau) , \tag{4.8a}$$

$$\dot{\mathcal{F}}_0(\omega, \tau) = -\omega\Theta(-\omega) + \frac{1}{2\pi}\int_0^\infty ds\,\cos(\omega s)\left(-\frac{p'(\tau - d)p'(\tau - d - s)}{[p(\tau - d) - p(\tau - d - s)]^2} + \frac{1}{s^2}\right) , \tag{4.8b}$$

$$\dot{\mathcal{F}}_1(\omega, \tau) = \frac{1}{2\pi}\int_0^\infty ds\,\frac{\cos(\omega s)\,p'(\tau - d - s)}{[\tau + d - p(\tau - d - s)]^2} , \tag{4.8c}$$

$$\dot{\mathcal{F}}_2(\omega, \tau) = \frac{1}{2\pi}\int_0^\infty ds\,\text{Re}\left(\frac{\text{e}^{-\text{i}\omega s}\,p'(\tau - d)}{[p(\tau - d) - \tau - d + s - \text{i}\epsilon]^2}\right) . \tag{4.8d}$$

In (4.8b) and (4.8c) we have set $\epsilon = 0$ as the integrand has no singularities. The ϵ in (4.8d) needs to be kept as the integrand has a singularity, arising because the points $\tau - s$ and τ on the detector's trajectory are connected by a null ray that is reflected from the mirror, as shown in Figure 1. The integral is well defined despite this singularity since the switch-on is in the asymptotic past so that the range of s cannot end at the singularity.

17

We show in Appendix C that the early and late time forms of the transition rate (4.8) are

$$\dot{\mathcal{F}}(\omega, \tau) = -\omega\left[1 - \cos(2d\omega)\right]\Theta(-\omega) + O(e^{\kappa\tau}) \qquad \text{as } \tau \to -\infty \,, \tag{4.9a}$$

$$\dot{\mathcal{F}}(\omega, \tau) = -\frac{\omega}{2}\Theta(-\omega) + \frac{\omega}{2\left(e^{2\pi\omega/\kappa} - 1\right)} + o(1) \qquad \text{as } \tau \to \infty \,. \tag{4.9b}$$

4.3 Inertial detector: travelling towards the mirror in the distant past

We next consider a detector on the inertial worldline

$$\mathsf{x}(\tau) = (\tau\cosh\lambda, -\tau\sinh\lambda) \,, \tag{4.10}$$

where $\lambda > 0$. In the asymptotic past, where the mirror is static, the detector is moving towards the mirror with speed $\tanh\lambda$.

Proceeding as above, we find

$$\dot{\mathcal{F}}(\omega, \tau) = \dot{\mathcal{F}}_0(\omega, \tau) + \dot{\mathcal{F}}_1(\omega, \tau) + \dot{\mathcal{F}}_2(\omega, \tau) \,, \tag{4.11a}$$

$$\dot{\mathcal{F}}_0(\omega, \tau) = -\omega\Theta(-\omega) + \frac{1}{2\pi}\int_0^\infty ds\,\cos(\omega s)\left(-\frac{p'(e^\lambda\tau)p'\left(e^\lambda(\tau - s)\right)e^{2\lambda}}{\left[p(e^\lambda\tau) - p\left(e^\lambda(\tau - s)\right)\right]^2} + \frac{1}{s^2}\right) \,, \tag{4.11b}$$

$$\dot{\mathcal{F}}_1(\omega, \tau) = \frac{1}{2\pi}\int_0^\infty ds\,\frac{\cos(\omega s)\,p'\left(e^\lambda(\tau - s)\right)}{\left[e^{-\lambda}\tau - p\left(e^\lambda(\tau - s)\right)\right]^2} \,, \tag{4.11c}$$

$$\dot{\mathcal{F}}_2(\omega, \tau) = \frac{1}{2\pi}\int_0^\infty ds\,\text{Re}\left(\frac{e^{-i\omega s}\,p'(e^\lambda\tau)}{\left[p(e^\lambda\tau) - e^{-\lambda}(\tau - s) - i\epsilon\right]^2}\right) \,, \tag{4.11d}$$

and we show in Appendix C that the early and late time forms are

$$\dot{\mathcal{F}}(\omega, \tau) = -\omega\left[1 - e^{2\lambda}\cos(2\tau\sinh\lambda\,e^\lambda\omega)\right]\Theta(-\omega) + O(\tau^{-1}) \qquad \text{as } \tau \to -\infty \,, \tag{4.12a}$$

$$\dot{\mathcal{F}}(\omega, \tau) = -\frac{\omega}{2}\Theta(-\omega) + \frac{\omega}{2\left(e^{2\pi e^{-\lambda}\omega/\kappa} - 1\right)} + o(1) \qquad \text{as } \tau \to \infty \,. \tag{4.12b}$$

4.4 Onset of thermality

We are now ready to discuss the sense in which the transition rate exhibits the onset of thermality as the mirror continues to recede.

Consider first the distant past. For the detector (3.1), static with respect to the mirror, the transition rate (4.9a) agrees with that (3.7b) of the same detector in the static half-space $\widetilde{\mathcal{M}}$. For the detector (4.10), drifting towards the mirror, the transition rate (4.12a) can be verified to agree with that of the same detector in $\widetilde{\mathcal{M}}$. Compared

with (4.9a), the non-Minkowski part of (4.12a) has the static distance d replaced by the time-dependent distance $-\tau \sinh \lambda$, ω replaced by the blueshifted frequency $\mathrm{e}^\lambda \omega$, and an additional blueshift factor e^λ.

Consider then the distant future. The distant future transition rates (4.9b) and (4.12b) agree with the transition rate (3.18) of an inertial detector in Minkowski space when the left-movers are in the Minkowski vacuum and the right-movers are thermal in temperature $\kappa/(2\pi)$. Note that the detector's velocity shows up by a Doppler blueshift in the right-mover contribution.

The late time transition rates (4.9b) and (4.12b) can hence be interpreted to consist of a contribution from the left-moving part of the field, undisturbed by the mirror, and and a contribution from the right-moving part of the field, excited by the mirror to induce a Planckian response. This interpretation is consistent with the fact that the stress-energy tensor of the field contains at late times an energy flux to the right [1, 28, 29, 50, 51].

This late time result is consistent with that quoted in [1] for a non-derivative UDW detector with a mirror trajectory with similar late time asymptotics, in the sense that the left-mover contribution was not explicitly written out in [1].

Figures 2 and 3 show numerical plots for the evolution of the transition rate from early to late times, for the detector (3.1) that is static with respect to the mirror in the distant past. The asymptotic late time value is reached via a ring-down of oscillations whose period equals $2\pi/\kappa$ within the range of the numerical experiments. We have not attempted to examine this oscillation analytically.

5 $(1+1)$ Schwarzschild spacetime

In this section we consider a detector in the $(1+1)$-dimensional Schwarzschild spacetime, obtained by dropping the angular dimensions from the $(3+1)$-dimensional Schwarzschild metric [52]. We first establish the notation, recall the definitions of the Boulware, HHI and Unruh vacua [1], and discuss briefly the case of a static detector in the exterior. The main objective is to study a geodesically infalling detector.

5.1 Spacetime and vacua

We write the metric of the $(1+1)$-dimensional maximally extended Schwarzschild spacetime in the notation of [1] as

$$ds^2 = -\frac{2M\mathrm{e}^{-r/(2M)}}{r}\, d\bar{u}\, d\bar{v} \ , \tag{5.1}$$

where $M > 0$ is the Schwarzschild mass parameter, the Kruskal null coordinates $\bar{u}$ and $\bar{v}$ increase towards the future and satisfy $\bar{u}\bar{v} < (4M)^2$, and $r \in \mathbb{R}_+$ is the unique solution to

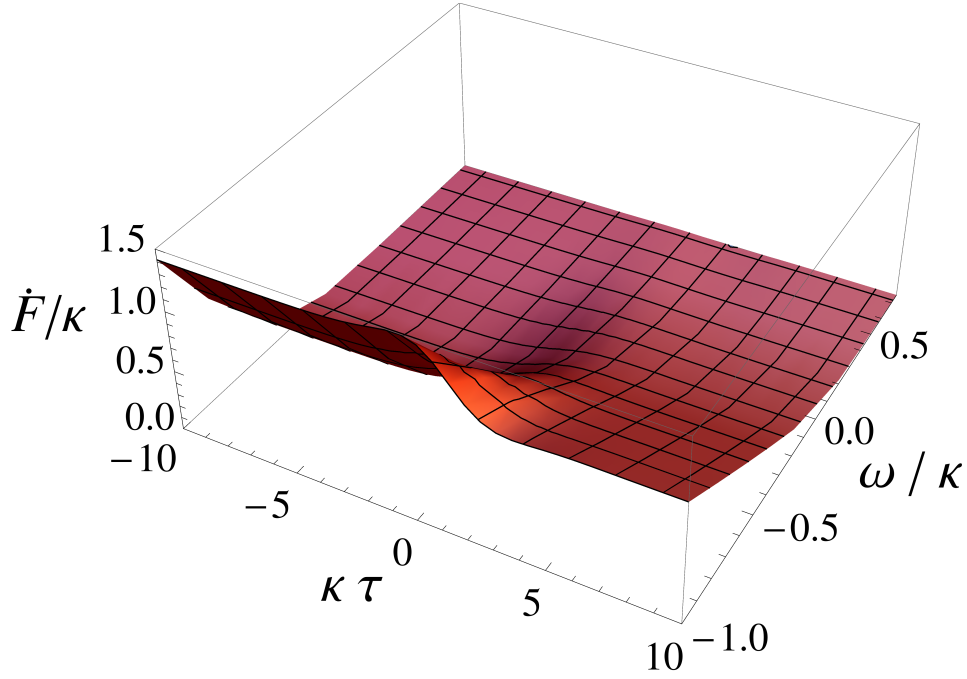$$-\bar{u}\bar{v} = (4M)^2 \big[r/(2M) - 1\big] e^{r/(2M)} \ . \tag{5.2}$$

Figure 2: The figure shows a perspective plot of the transition rate $\dot{\mathcal{F}}(\omega, \tau)$ (4.8) for the detector (3.1) that is asymptotically static with respect to the mirror in the distant past, with $d = 1/\kappa$.
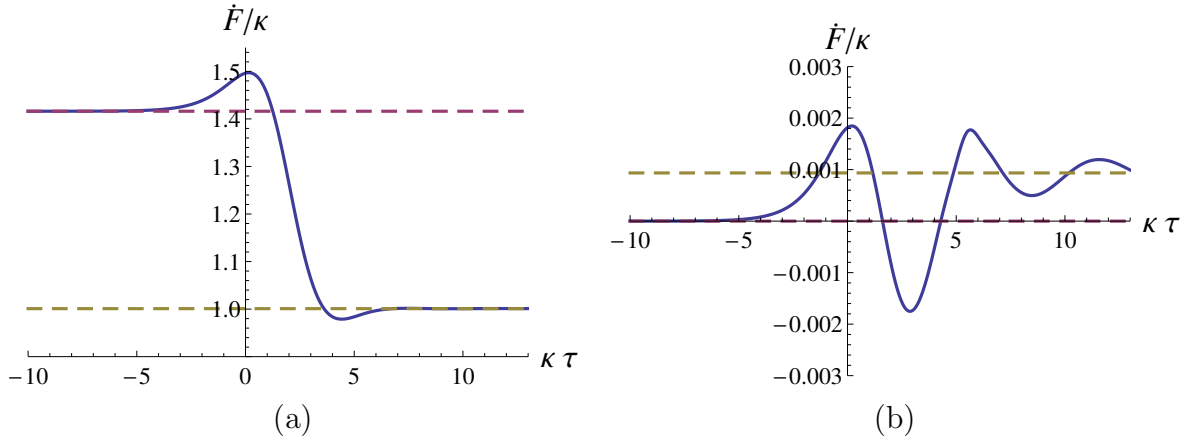

Figure 3: Cross-sections of the plot in Figure 2 at (a) $\omega = -\kappa$ and (b) $\omega = \kappa$. The dashed horizontal lines show the past and future asymptotic values (4.9).

The metric has the Killing vector $\xi = (4M)^{-1}(-\bar{u}\partial_{\bar{u}} + \bar{v}\partial_{\bar{v}})$, which is timelike for $\bar{u}\bar{v} < 0$ ($r > 2M$), spacelike for $\bar{u}\bar{v} > 0$ ($r < 2M$) and null at the Killing horizon $\bar{u}\bar{v} = 0$ ($r = 2M$). The right-going (respectively left-going) branch of the Killing horizon is $\bar{u} = 0$ ($\bar{v} = 0$). The Killing horizon divides the spacetime into four quadrants as summarised in Table 1.

We denote by u and v the tortoise null coordinates defined by

$$u = -4M \ln[-\bar{u}/(4M)] \qquad \text{for } \bar{u} < 0 , \tag{5.3a}$$

$$v = 4M \ln[\bar{v}/(4M)] \qquad \text{for } \bar{v} > 0 . \tag{5.3b}$$

In Quadrant I (right-hand exterior), where $r > 2M$, we can hence introduce the usual exterior Schwarzschild coordinates (t, r) by

$$u = t - r - 2M \ln[r/(2M) - 1] , \tag{5.4a}$$
$$v = t + r + 2M \ln[r/(2M) - 1] , \tag{5.4b}$$

so that

$$t = 2M \ln(-\bar{v}/\bar{u}) , \tag{5.5}$$

the metric reads

$$ds^2 = -(1 - 2M/r)\, dt^2 + \frac{dr^2}{(1 - 2M/r)} , \tag{5.6}$$

and $\xi = \partial_t$. In Quadrant II, where $r < 2M$, we can similarly introduce the Schwarzschild-like coordinates $(\tilde{t}, r)$ by (5.2) and

$$\tilde{t} = 2M \ln(\bar{v}/\bar{u}) , \tag{5.7}$$

so that the metric takes the form

$$ds^2 = -\frac{dr^2}{[(2M/r) - 1]} + [(2M/r) - 1]\, d\tilde{t}^2 \tag{5.8}$$

Quadrant	$\bar{u}$	$\bar{v}$	$\xi^a \xi_a$	r
I: right-hand exterior	$-$	$+$	$-$	$2M < r < \infty$
II: black hole interior	$+$	$+$	$+$	$0 < r < 2M$
III: left-hand exterior	$+$	$-$	$-$	$2M < r < \infty$
IV: white hole interior	$-$	$-$	$+$	$0 < r < 2M$

Table 1: The four quadrants of the extended Schwarzschild spacetime. The columns show the signs of the Kruskal coordinates $\bar{u}$ and $\bar{v}$, the norm squared of the Killing vector ξ, and the range of the function r. In the exteriors, where ξ is timelike, it is future-pointing in Quadrant I and past-pointing in Quadrant III.

and $\xi = \partial_{\tilde{t}}$. A pair of coordinates that covers Quadrants I and II and the black hole horizon that separates them is $(\bar{u}, v)$. We shall not need the explicit form of the metric in these coordinates.

We consider a massless minimally coupled scalar field in three distinguished states. First, in Quadrant I we consider the Boulware vacuum $|0_B\rangle$, defined by the positive and negative frequency decomposition with respect to ∂_t in (5.6) [53]. At the asymptotically flat infinity of Quadrant I, $|0_B\rangle$ reduces to the Minkowski vacuum. Second, on the whole spacetime we consider the HHI vacuum $|0_H\rangle$, defined by the positive and negative frequency decomposition with respect to $\partial_{\bar{u}}$ and $\partial_{\bar{v}}$ on the Killing horizon [54, 55]. In Quadrant I, $|0_H\rangle$ is a thermal equilibrium state with respect to ∂_t, at the local Hawking temperature

$$T_{\text{loc}} = \frac{1}{8\pi M \sqrt{1 - 2M/r}} \ . \tag{5.9}$$

Third, in Quadrants I and II and on the black hole horizon that separates them, we consider the Unruh vacuum $|0_U\rangle$, defined by the positive and negative frequency decomposition with respect to $\partial_{\bar{u}}$ and ∂_v in the coordinates $(\bar{u}, v)$ [3]. $|0_U\rangle$ mimics a state that results from the collapse of a star at late times when there is initially no incoming radiation from infinity, and it has the left-moving part of the field in a Boulware-like state and the right-moving part of the field in a HHI-like state.

The Wightman functions for the three vacua are [1]

$$\langle 0_B | \phi(\mathsf{x}) \phi(\mathsf{x}') | 0_B \rangle = -\frac{1}{4\pi} \ln[(\epsilon + \mathrm{i}\Delta u)(\epsilon + \mathrm{i}\Delta v)] \ , \tag{5.10a}$$

$$\langle 0_H | \phi(\mathsf{x}) \phi(\mathsf{x}') | 0_H \rangle = -\frac{1}{4\pi} \ln[(\epsilon + \mathrm{i}\Delta \bar{u})(\epsilon + \mathrm{i}\Delta \bar{v})] \ , \tag{5.10b}$$

$$\langle 0_U | \phi(\mathsf{x}) \phi(\mathsf{x}') | 0_U \rangle = -\frac{1}{4\pi} \ln[(\epsilon + \mathrm{i}\Delta \bar{u})(\epsilon + \mathrm{i}\Delta v)] \ , \tag{5.10c}$$

where $\Delta u = u - u'$ and similarly for the other coordinates. Each of the Wightman functions is unique up to a real-valued additive constant. The Boulware and HHI vacuum Wightman functions are invariant under the isometries generated by the Killing vector ξ. The Unruh vacuum Wightman function changes under these isometries by an additive constant; however, the Unruh vacuum may nevertheless be considered invariant under the isometries since the stress-energy tensor and other quantities built from derivatives of the Wightman function are invariant [31, 32]. The non-invariance of the Unruh vacuum Wightman function is due to the infrared properties of the (1+1)-dimensional conformal field and has no counterpart in higher dimensions [56].

5.2 Static detector

We consider first a detector in Quadrant I on the static, noninertial trajectory $r = R$, where $R > 2M$ is a constant. Using (2.17) and (5.10), the calculations are closely similar

to those in Section 3, and we omit the detail. We find

$$\dot{\mathcal{F}}_B(\omega) = -\omega\Theta(-\omega) \ , \tag{5.11a}$$

$$\dot{\mathcal{F}}_H(\omega) = \frac{\omega}{e^{\omega/T_{\text{loc}}} - 1} \ , \tag{5.11b}$$

$$\dot{\mathcal{F}}_U(\omega) = -\frac{\omega}{2}\Theta(-\omega) + \frac{\omega}{2\left(e^{\omega/T_{\text{loc}}} - 1\right)} \ , \tag{5.11c}$$

for respectively the Boulware, HHI and Unruh vacua, where T_{loc} is the local Hawking temperature (5.9) evaluated at $r = R$.

These results conform fully to expectations. The Boulware vacuum transition rate is that of an inertial detector in Minkowski space in Minkowski vacuum, while the HHI vacuum transition rate is thermal in the local Hawking temperature (5.9). The Unruh vacuum transition rate is the average of the two, with the two pieces arising respectively from the left-moving and right-moving parts of the field.

These results are also consistent with what was reported for the non-derivative UDW detector in [1], in the sense that the left-mover contribution in (5.11c) was not explicitly written out in [1]. Finally, the similarity between (5.11c) and our receding mirror spacetime results (4.9b) and (4.12b) is an additional confirmation that the Unruh vacuum mimics the late time properties of a state created in a collapsing star spacetime [1, 3].

5.3   Interlude: geodesics

We next turn to inertial detectors. In this subsection we recall a convenient parametrisation for the geodesics. We give the full expressions in a form that applies only to Quadrant I, where the equations of a timelike geodesic in the Schwarzschild coordinates (5.6) take the form

$$\dot{t} = \frac{E}{1 - 2M/r} \ , \tag{5.12a}$$

$$\dot{r}^2 = E^2 - 1 + 2M/r \ , \tag{5.12b}$$

where E is a positive constant and the overdot denotes derivative with respect to the proper time τ. The continuation beyond Quadrant I can be done by passing to the Kruskal coordinates $(\bar{u}, \bar{v})$.

When $E > 1$, the geodesic has at infinity the nonvanishing speed $\sqrt{1 - E^{-2}}$ with respect to the Killing vector ξ. We consider a geodesic that is sent in from the infinity,

so that $\dot{r} < 0$. The geodesic can be parametrised as

$$\tau = \frac{M}{(E^2 - 1)^{3/2}} \left(\sinh \chi - \chi \right) , \tag{5.13a}$$

$$r = \frac{M}{(E^2 - 1)} \left(\cosh \chi - 1 \right) , \tag{5.13b}$$

$$t = \frac{ME}{(E^2 - 1)^{3/2}} \left[\sinh \chi + (2E^2 - 3)\chi \right] + 2M \ln \left(\frac{-\tanh(\chi/2) + \sqrt{1 - E^{-2}}}{-\tanh(\chi/2) - \sqrt{1 - E^{-2}}} \right) , \tag{5.13c}$$

where the parameter χ takes values in $(-\infty, 0)$, so that the trajectory starts at the infinity in the asymptotic past at $\chi \to -\infty$ and hits the singularity at $\chi \to 0$. The additive constant in (5.13a) is chosen so that $-\infty < \tau < 0$. The horizon-crossing occurs at $\chi = \chi_h \doteq -2 \operatorname{arctanh}\left(\sqrt{1 - E^{-2}} \right)$. Equation (5.13c) applies only in Quadrant I, where $-\infty < \chi < \chi_h$.

When $E = 1$, the geodesic has at infinity a vanishing speed with respect to ξ. We consider again a geodesic that is sent in from the infinity. The geodesic takes the form

$$r = 2M[-3\tau/(4M)]^{2/3} , \tag{5.14a}$$

$$t = \tau - 4M[-3\tau/(4M)]^{1/3} + 2M \ln \left(\frac{[-3\tau/(4M)]^{1/3} + 1}{[-3\tau/(4M)]^{1/3} - 1} \right) , \tag{5.14b}$$

where $-\infty < \tau < 0$. The horizon-crossing occurs at $\tau = \tau_h \doteq -4M/3$, and the singularity is reached as $\tau \to 0$. Equation (5.14b) applies only in Quadrant I, where $-\infty < \tau < \tau_h$.

When $0 < E < 1$, the geodesic has a maximum value of r. The geodesic can be parametrised as

$$\tau = \frac{M}{(1 - E^2)^{3/2}} \left(\varphi + \sin \varphi \right) , \tag{5.15a}$$

$$r = \frac{M}{(1 - E^2)} \left(1 + \cos \varphi \right) , \tag{5.15b}$$

$$t = \frac{ME}{(1 - E^2)^{3/2}} \left[\sin \varphi + (3 - 2E^2)\varphi \right] + 2M \ln \left(\frac{1 + \sqrt{E^{-2} - 1} \, \tan(\varphi/2)}{1 - \sqrt{E^{-2} - 1} \, \tan(\varphi/2)} \right) , \tag{5.15c}$$

where the parameter φ takes values in $(-\pi, \pi)$, so that the trajectory starts at the white hole singularity at $\varphi \to -\pi$ and ends at the black hole singularity at $\varphi \to \pi$. The additive constant in (5.15a) is chosen so that $\tau = 0$ at the moment when r reaches its maximum value, $2M/(1 - E^2)$. The total proper time elapsed between the singularities is $2\pi M(1 - E^2)^{-3/2}$. The horizon-crossings occur at $\varphi = \mp\varphi_h$ where

$\varphi_h \doteq 2 \arctan\left(\sqrt{E^{-2} - 1}\,\right)$. Equation (5.15c) applies only in Quadrant I, where $-\varphi_h < \varphi < \varphi_h$.

Finally, there exist also timelike geodesics that pass from the white hole to the black hole through the horizon bifurcation point $\bar{u} = \bar{v} = 0$, without entering Quadrant I (or Quadrant III). These geodesics take the form

$$\bar{u} = \bar{v} = 4M \sin(\varphi/2) \exp\left[\tfrac{1}{2} \cos^2(\varphi/2)\right] , \qquad (5.16)$$

where the parameter φ takes values in $(-\pi, \pi)$, and τ and r are given by (5.15a) and (5.15b) with $E = 0$. The isometry generated by ξ has been used in (5.16) to set $\bar{u} = \bar{v}$ without loss of generality.

5.4 Inertial detector

The transition rate of the inertial detector is obtained by inserting the Wightman functions (5.10) and the geodesic trajectories of subsection 5.3 into the integral formulas of subsection 2.3. The transition rate is expressible as the integral of an elementary function for all values of E; for $E > 1$ (respectively $E < 1$) this is accomplished by writing the differentiations and the integration in terms of $\chi\,(\varphi)$.

We address the near-infinity and near-singularity limits analytically and the intermediate regime numerically.

5.4.1 Near the infinity

We consider the $E > 1$ trajectories (5.13) and the $E = 1$ trajectory (5.14), all of which fall in from the infinity, and we push the switch-on to the infinite past. It is shown in Appendix D that at early times, $\tau \to -\infty$, we have

$$\dot{\mathcal{F}}_B(\omega, \tau) = -\omega\Theta(-\omega) + o(1) , \qquad (5.17a)$$

$$\dot{\mathcal{F}}_H(\omega, \tau) = \frac{\omega}{2\left(e^{\omega/T_-} - 1\right)} + \frac{\omega}{2\left(e^{\omega/T_+} - 1\right)} + o(1) , \qquad (5.17b)$$

$$\dot{\mathcal{F}}_U(\omega, \tau) = -\frac{\omega}{2}\Theta(-\omega) + \frac{\omega}{2\left(e^{\omega/T_+} - 1\right)} + o(1) , \qquad (5.17c)$$

where $T_\pm \doteq e^{\pm\lambda}/(8\pi M)$ and $\lambda \doteq \operatorname{arctanh}\left(\sqrt{1 - E^{-2}}\,\right)$. For $E = 1$, we have $T_+ = T_- = 1/(8\pi M)$, so that the two terms in (5.17b) are equal and combine to the Planckian response.

The asymptotic past results (5.17) conform fully to physical expectations. The Boulware vacuum transition rate is that in Minkowski vacuum (3.7a), consistently with the interpretation of the Bouware vacuum as the no-particle state with respect to ξ. The HHI vacuum transition rate is that of an inertial detector in a thermal bath in Minkowski space (3.16), with the temperature given by the Hawking temperature at the infinity, $1/(8\pi M)$, and with each of the two Planckian terms containing a Doppler

25

shift factor that accounts for the detector's velocity at the infinity. The Unruh vacuum transition rate sees a Planckian term only in the outgoing part of the field, as confirmed by the Doppler shift to the blue in this term, while the term that corresponds to the ingoing part of the field is Minkowski-like.

5.4.2 Near the singularity

We consider the transition rate in the HHI and Unruh vacua in the limit where the detector approaches the black black hole singularity. We allow all values of the non-negative constant E. We also allow the switch-on moment to remain arbitrary, subject only to the condition that for $0 \leq E < 1$ the switch-on in the HHI vacuum takes place after the trajectory emerges from the white hole singularity, and the switch-on in the Unruh vacuum takes place after the trajectory crosses the past horizon.

It is shown in Appendix D that in this near-singularity limit we have

$$\dot{\mathcal{F}}(\omega, \tau) = \frac{1}{8\pi M} \left[\left(\frac{2M}{r(\tau)} \right)^{3/2} + \frac{1+E^2}{2} \left(\frac{2M}{r(\tau)} \right)^{1/2} \right] + O(1) , \qquad (5.18)$$

for both the HHI vacuum and the Unruh vacuum: the differences between the two vacua show up only in the $O(1)$ part. In terms of τ, the leading term in (5.18) is $1/[6\pi(\tau_{\text{sing}} - \tau)]$, where τ_{sing} is the value of τ at the black hole singularity.

5.4.3 Intermediate regime: loss of thermality

For a trajectory falling in from the infinity in the HHI and Unruh vacua, it is seen from the limits (5.17) and (5.18) that the thermal character of the transition rate is lost during the infall. Numerical evidence of how this loss takes place for the $E = 1$ trajectory is shown in Figures 4 and 5. The numerical evidence shows that the Planckian form of the transition rate is lost before the trajectory crosses the horizon.

Numerical evidence also corroborates that the overall magnitude of the transition rate increases during the infall and grows without bound near the singularity. A sample plot for the $E = 1$ trajectory in the HHI vacuum is shown in Figure 6.

Finally, suppose the field is in the HHI vacuum, and consider the trajectory that passes from the white hole to the black hole through the horizon bifurcation point. We use the parametrisation (5.16), so that (5.15a) and (5.15b) hold with $E = 0$. We switch the detector on at $\varphi = -9\pi/10$, close to but well separated from the white hole singularity at $\varphi = -\pi$. Figure 7 shows a perspective plot of the transition rate as a function of ω and τ. The plot shows clearly both the divergence when τ approaches the switch-on time, arising from the last term in (2.14), and the divergence when the trajectory approaches the black hole singularity.

To examine the thermal character of the transition rate, we have evaluated numerically the quantity

$$T_{\text{as,KMS}}(\omega, \tau) \doteq \frac{\omega}{\ln\big(\dot{\mathcal{F}}(-\omega, \tau)/\dot{\mathcal{F}}(\omega, \tau)\big)} . \qquad (5.19)$$
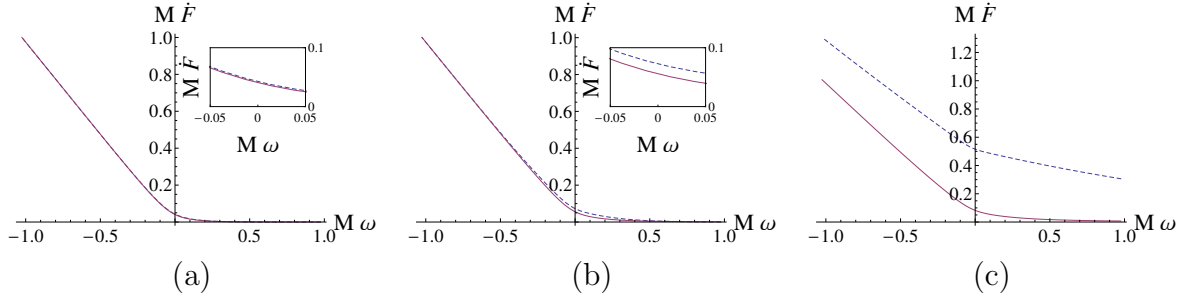
26

Figure 4: The solid (red) curve shows $M\dot{\mathcal{F}}$ as a function of $M\omega$ for the $E = 1$ trajectory in the HHI vacuum, at the times (a) $\tau = -10M$, (b) $\tau = -3.5M$ and (c) $\tau = -1.5M$, all of them before the horizon-crossing, which occurs at $\tau = \tau_h = -(4/3)M$. The dashed (blue) curve shows M times the Minkowski thermal bath response (3.16) at the local Hawking temperature T_{loc} (5.9) and with the Doppler shift factor $\lambda = \lambda_{\mathrm{loc}} = \mathrm{arctanh}\left(\sqrt{2M/r}\right)$, as a function of $M\omega$. The discrepancy between the two curves shows that the Planckian character of the transition rate is lost as τ approaches τ_h, where the solid curve remains finite but the dashed curve disappears to $+\infty$.
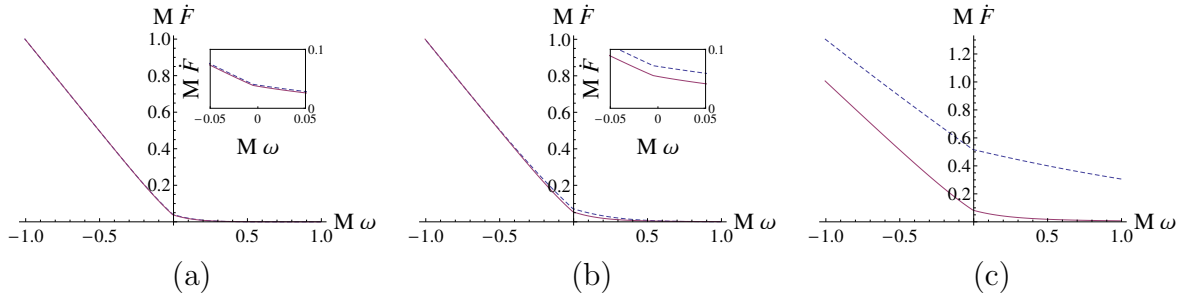

Figure 5: The solid (red) curve is as in Figure 4 but for the Unruh vacuum. The dashed (blue) curve shows M times the Minkowski response (3.18) in a state with vacuum left-movers and thermal right-movers, at the local Hawking temperature T_{loc} (5.9) and with the Doppler shift factor $\lambda = \lambda_{\mathrm{loc}} = \mathrm{arctanh}\left(\sqrt{2M/r}\right)$. The discrepancy between the two curves again shows loss of the Planckian character as τ approaches τ_h, where the solid curve remains finite but the dashed curve disappears to $+\infty$. Note the discontinuous slope of the dashed curve at $\omega = 0$.
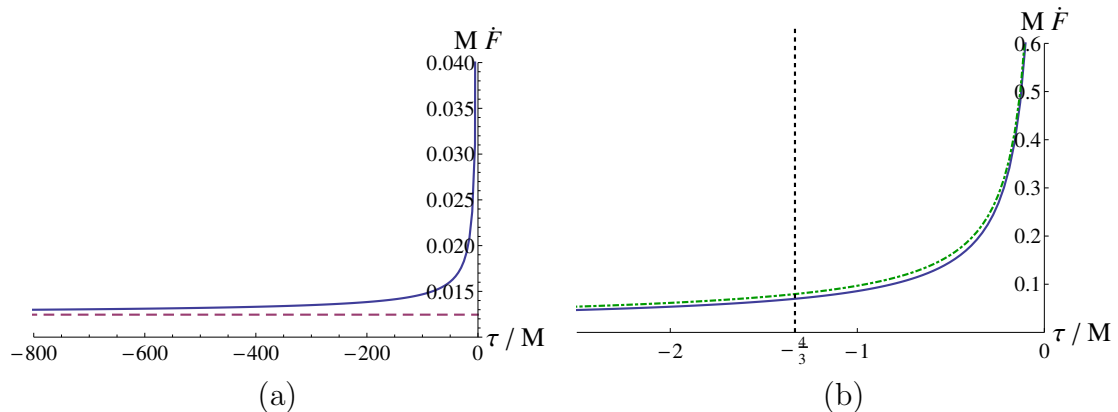
Figure 6: (a) The solid (blue) curve shows $M\dot{\mathcal{F}}\big(1/(4\pi M)\big)$ as a function of τ/M for the $E = 1$ trajectory in the HHI vacuum. The dashed (red) line shows the value $1/[4\pi(\mathrm{e}^2-1)]$ to which the solid curve asymptotes at $\tau/M \to -\infty$. (b) The solid (blue) curve shows a close-up of (a) near the horizon-crossing, $\tau/M = -4/3$. The dash-dotted (green) curve shows the τ-dependent terms included in the asymptotic $\tau \to 0$ expression (5.18).
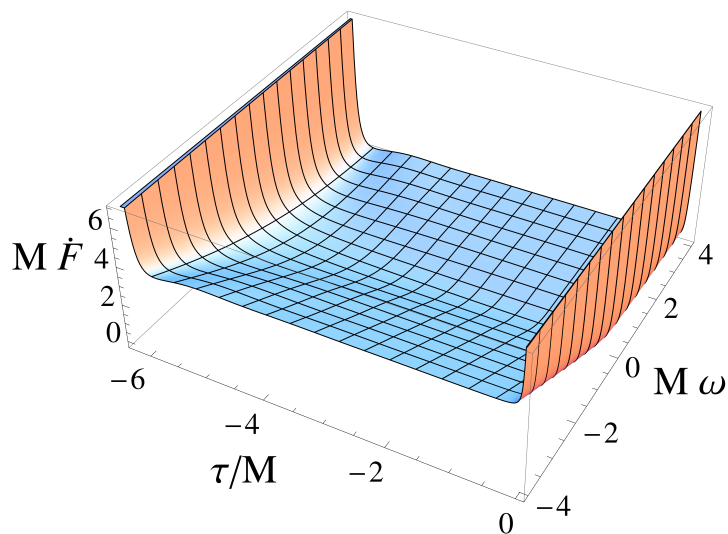

Figure 7: The transition rate for a detector on the $E = 0$ trajectory (5.16) in the HHI vacuum, with the switch-on at $\varphi = -9\pi/10$, where $\tau \approx -3.136M$. The white hole singularity is at $\varphi = -\pi$, where $\tau = -\pi M$. The divergence of the transition rate in the limit of short detection time and in the limit of approaching the black hole singularity is evident in the plot.

28

If $T_{\mathrm{as,KMS}}$ were (approximately) independent of ω for fixed τ, the transition rate would satisfy (approximately) the KMS condition (3.11) and $T_{\mathrm{as,KMS}}$ would be equal to (approximate) KMS temperature, which could possibly be τ-dependent. Within the parameter range that our numerical experiments have been able to probe, we have however found no regimes in which $T_{\mathrm{as,KMS}}$ would be (approximately) independent of ω.

6   Conclusions

In this paper we have analysed an UDW detector that is coupled to the proper time derivative of a scalar field in a $(1+1)$-dimensional spacetime. Working within first-order perturbation theory, we showed that although the derivative makes the interaction between the detector and the field more singular, the singularity is no worse than that of the non-derivative UDW detector in $(3+1)$ spacetime dimensions, and issues of switching can be handled by the same techniques. In particular, even though the transition probability diverges in the sharp switching limit, the transition rate remains well defined and allows the detector to address strongly time-dependent situations.

Our main aim was to show that the derivative-coupling detector provides a viable tool for probing a $(1+1)$-dimensional massless field, whose infrared properties create ambiguities for the conventional UDW detector in time-dependent situations. We presented strong evidence that the derivative-coupling detector does remain well-behaved for the massless field, with and without time-dependence. As specific time-dependent examples, we analysed an inertial detector in a Minkowski spacetime with an exponentially receding mirror and a detector falling inertially into the $(1+1)$-dimensional Schwarzschild black hole. In both cases we recovered the expected thermal results due to the Hawking-Unruh effect in the appropriate limits. In the receding mirror spacetime we saw the thermality gradually set in as the mirror's acceleration approaches the asymptotic late time behaviour, tailored to model the late time effects of a gravitational collapse. In the $(1+1)$-dimensional Schwarzschild spacetime we saw thermality gradually lost as the detector falls, and we saw the transition rate diverge as the detector approaches the black hole singularity, for both the HHI and Unruh vacua.

Our results about the time-dependence of the Hawking-Unruh effect complement those obtained via Bogoliubov coefficient techniques or via a quasi-temperature approximation to the Wightman function [57, 58, 59, 60]. A key input in our analysis was to characterise the time-dependence of the response in terms of the instantaneous transition rate, defined by taking the sharp switching limit, and mathematically well defined in our spacetimes even when the time-dependence is strong. A conceptual disadvantage of the instantanous transition rate is however that it cannot be measured by a single detector, or even by an ensemble of detectors, but the measurement requires an ensemble of ensembles of detectors [12, 15]. A technical disadvantage is that the instantanous transition rate becomes singular when the Wightman function has singularities that typically occur with spatial periodicity [37]. Further, the limit of sharp switching and the limit of large energy gap need not commute [61], which becomes an issue when one

attempts to identify characteristics of thermal behaviour in the response of a detector that operates for a genuinely finite interval of time. While we hence do not advocate the instantaneous transition rate as a definitive quantifier of time-dependence in the detector's response, our results strongly suggest that the instantaneous transition rate conveys a physically expected picture about the onset and decay of the Hawking-Unruh effect.

Acknowledgments

A   Evaluation of $\mathcal{F}_{\mathrm{sing}}$ (2.6c)

In this appendix we show that $\mathcal{F}_{\mathrm{sing}}$ (2.6c) can be written as (A.6) or (A.7).

Starting from (2.6c) and integrating the distributional derivatives by parts, we have

$$\mathcal{F}_{\mathrm{sing}}(\omega) = \int_{-\infty}^{\infty} d\tau' \int_{-\infty}^{\infty} d\tau'' \, Q'_{\omega}(\tau')\overline{Q'_{\omega}(\tau'')} \, \mathcal{W}_{\mathrm{sing}}(\tau', \tau'') \; , \tag{A.1}$$

where $Q_{\omega}(\tau) \doteq \mathrm{e}^{-\mathrm{i}\omega\tau}\chi(\tau)$ and the prime denotes derivative with respect to the argument. Note that the integrand in (A.1) is a locally integrable function, containing no distributional parts. Using the explicit form of $\mathcal{W}_{\mathrm{sing}}$ (2.4), we obtain

$$\mathcal{F}_{\mathrm{sing}}(\omega) = \mathcal{F}_{\mathrm{sing},1}(\omega) + \mathcal{F}_{\mathrm{sing},2}(\omega) \; , \tag{A.2a}$$

$$\mathcal{F}_{\mathrm{sing},1}(\omega) = -\frac{\mathrm{i}}{4} \int_{-\infty}^{\infty} d\tau' \int_{-\infty}^{\infty} d\tau'' \, Q'_{\omega}(\tau')\overline{Q'_{\omega}(\tau'')} \, \mathrm{sgn}(\tau' - \tau'') \; , \tag{A.2b}$$

$$\mathcal{F}_{\mathrm{sing},2}(\omega) = -\frac{1}{2\pi} \int_{-\infty}^{\infty} d\tau' \int_{-\infty}^{\infty} d\tau'' \, Q'_{\omega}(\tau')\overline{Q'_{\omega}(\tau'')} \, \ln|\tau' - \tau''| \; . \tag{A.2c}$$

For $\mathcal{F}_{\text{sing},1}$, integrating over τ'' in (A.2b) gives

$$\mathcal{F}_{\text{sing},1}(\omega) = -\frac{\mathrm{i}}{2} \int_{-\infty}^{\infty} du\, Q'_\omega(u)\overline{Q_\omega(u)}$$

$$= -\frac{\mathrm{i}}{2} \int_{-\infty}^{\infty} du\, [\chi'(u) - \mathrm{i}\omega\chi(u)]\,\chi(u)$$

$$= -\frac{\omega}{2} \int_{-\infty}^{\infty} du\, [\chi(u)]^2 \,, \tag{A.3}$$

where we have renamed τ' as u, used the definition of Q_ω, and finally noted that $\int_{-\infty}^{\infty} du\, \chi'(u)\chi(u) = \frac{1}{2}\int_{-\infty}^{\infty} du\, \frac{d}{du}[\chi(u)]^2 = 0$.

For $\mathcal{F}_{\text{sing},2}$, we break the integral in (A.2c) into the subdomains $\tau' > \tau''$ and $\tau' < \tau''$. In the subdomain $\tau' > \tau''$ we write $\tau' = u$ and $\tau'' = u - s$, where $u \in \mathbb{R}$ and $0 < s < \infty$, and in the subdomain $\tau' < \tau''$ we write $\tau'' = u$ and $\tau' = u - s$, where again $u \in \mathbb{R}$ and $0 < s < \infty$. This gives

$$\mathcal{F}_{\text{sing},2}(\omega) = -\frac{1}{\pi} \int_0^{\infty} ds\, \ln s \int_{-\infty}^{\infty} du\, \mathrm{Re}\left[Q'_\omega(u)\overline{Q'_\omega(u-s)} \right]$$

$$= \frac{1}{\pi} \int_0^{\infty} ds\, \ln s \int_{-\infty}^{\infty} du\, \mathrm{Re}\left[Q_\omega(u)\overline{Q''_\omega(u-s)} \right]$$

$$= \frac{1}{\pi} \int_0^{\infty} ds\, \ln s\, \frac{d^2}{ds^2} \int_{-\infty}^{\infty} du\, \mathrm{Re}\left[Q_\omega(u)\overline{Q_\omega(u-s)} \right]$$

$$= \frac{1}{\pi} \int_0^{\infty} ds\, \ln s\, \frac{d^2}{ds^2} \left(\cos(\omega s) \int_{-\infty}^{\infty} du\, \chi(u)\chi(u-s) \right)$$

$$= -\frac{1}{\pi} \int_0^{\infty} \frac{ds}{s}\, \frac{d}{ds} \left(\cos(\omega s) \int_{-\infty}^{\infty} du\, \chi(u)\chi(u-s) \right) \,, \tag{A.4}$$

where we have first integrated by parts in u, then written the derivatives in $\overline{Q''_\omega(u-s)}$ as s-derivatives outside the u-integral, then used the definition of Q_ω, and finally integrated by parts in s. The substitution term from $s = 0$ in the integration by parts vanishes because $\cos(\omega s) \int_{-\infty}^{\infty} du\, \chi(u)\chi(u-s)$ is even in s, and the integral over s in the last expression in (A.4) is convergent at small s for the same reason.

In the last expression in (A.4), writing $\chi(u)\chi(u-s) = [\chi(u)]^2 - \chi(u)[\chi(u) - \chi(u-s)]$

31

gives

$$\mathcal{F}_{\text{sing},2}(\omega) = \frac{\omega}{\pi} \left(\int_{-\infty}^{\infty} du\, [\chi(u)]^2 \right) \int_0^{\infty} ds\, \frac{\sin(\omega s)}{s}$$

$$+ \frac{1}{\pi} \int_0^{\infty} \frac{ds}{s} \frac{d}{ds} \left(\cos(\omega s) \int_{-\infty}^{\infty} du\, \chi(u)[\chi(u) - \chi(u-s)] \right)$$

$$= \frac{|\omega|}{2} \int_{-\infty}^{\infty} du\, [\chi(u)]^2 + \frac{1}{\pi} \int_0^{\infty} ds\, \frac{\cos(\omega s)}{s^2} \int_{-\infty}^{\infty} du\, \chi(u)[\chi(u) - \chi(u-s)] \,,$$

$$(A.5)$$

where in the first term we have used the identity $\int_0^{\infty} ds\, s^{-1} \sin(\omega s) = \frac{1}{2}\pi \operatorname{sgn}\omega$, and in the second term we have integrated by parts. The integral over s in the second term is convergent at small s because $\int_{-\infty}^{\infty} du\, \chi(u)[\chi(u) - \chi(u-s)]$ vanishes at $s = 0$ and is even in s.

Combining (A.3) and (A.5), we obtain

$$\mathcal{F}_{\text{sing}}(\omega) = -\omega \Theta(-\omega) \int_{-\infty}^{\infty} du\, [\chi(u)]^2$$

$$+ \frac{1}{\pi} \int_0^{\infty} ds\, \frac{\cos(\omega s)}{s^2} \int_{-\infty}^{\infty} du\, \chi(u)[\chi(u) - \chi(u-s)] \,. \qquad (A.6)$$

An alternative expression is

$$\mathcal{F}_{\text{sing}}(\omega) = -\frac{\omega}{2} \int_{-\infty}^{\infty} du\, [\chi(u)]^2 + \frac{1}{\pi} \int_0^{\infty} \frac{ds}{s^2} \int_{-\infty}^{\infty} du\, \chi(u)\,[\chi(u) - \chi(u-s)]$$

$$+ \frac{1}{\pi} \int_{-\infty}^{\infty} du \int_0^{\infty} ds\, \chi(u)\chi(u-s) \frac{[1 - \cos(\omega s)]}{s^2} \,, \qquad (A.7)$$

which may be obtained from (A.6) by writing $\cos(\omega s) = 1 - [1 - \cos(\omega s)]$ and using the identity

$$\int_0^{\infty} ds\, \frac{1 - \cos(\omega s)}{s^2} = \frac{\pi|\omega|}{2} \,. \qquad (A.8)$$

B   Evaluation of the static detector's transition rate in Minkowski (half-)space

In this appendix we verify formulas (3.4) and (3.7) for the transition rate of a static detector in Minkowski space and Minkowski half-space. We use the Wightman functions found in subsection 3.1 and evaluate the transition rate from (2.17).

B.1 $m = 0$

We consider first the massless field, with the Wightman function given by (3.5) and (3.6).

In $\mathcal{M}$, we find from (2.8), (3.1) and (3.5) that $\mathcal{A}(\tau', \tau'') = -1/\big[2\pi(\tau' - \tau'' - \mathrm{i}\epsilon)^2\big]$. Evaluating (2.17) as a contour integral gives (3.7a).

In $\widetilde{\mathcal{M}}$, we find from (3.6) that the integrand in (2.17) contains the additional piece

$$\Delta\mathcal{A}(\tau', \tau'') = -\frac{\eta}{2\pi} \frac{(\tau' - \tau'' - \mathrm{i}\epsilon)^2 + 4d^2}{\big[(\tau' - \tau'' - \mathrm{i}\epsilon)^2 - 4d^2\big]^2} \; . \tag{B.1}$$

Evaluating the contribution to (2.17) as a contour integral leads to (3.7b).

We note that $\Delta\mathcal{A}(\tau', \tau'')$ (B.1) has distributional singularities at $\tau' - \tau'' = \pm 2d$. The geometric reason for these singularities is that the points τ' and τ'' on the detector's trajectory are connected by a null ray that is reflected from the mirror. As we have seen, the stationary transition rate is well defined despite these singularities. Were we however to consider a detector that operates for a finite duration, the singularities would interfere with the sharp switching limit manipulations that led to (2.14) when $\Delta\tau = 2d$.

B.2 $m > 0$

For the massive field, the Wightman function is given by (3.2) and (3.3). We consider $\mathcal{M}$ and $\widetilde{\mathcal{M}}$ in turn.

B.2.1 $\mathcal{M}$

In $\mathcal{M}$, we find from (2.8), (3.1) and (3.2) that

$$\mathcal{A}(\tau', \tau'') = \frac{m^2}{2\pi} K_0''\big[m\big(\epsilon + \mathrm{i}(\tau' - \tau'')\big)\big] \; , \tag{B.2}$$

where the prime denotes derivative with respect to the argument. From (2.17) we then obtain

$$\dot{\mathcal{F}}(\omega) = \frac{m^2}{2\pi} \int_C ds \, \mathrm{e}^{-\mathrm{i}\omega s} \, K_0''(\mathrm{i}ms) \; , \tag{B.3}$$

where the contour C in the complex s plane follows the real axis from $-\infty$ to $+\infty$ except that it drops in the lower half-plane near $s = 0$, and K_0 has its principal branch when s is negative imaginary. We now assume $\omega \neq -m$: it follows then from the asymptotics of K_0 at large imaginary argument [48] that (B.3) is convergent as an improper Riemann integral.

From (B.3) we obtain

$$\dot{\mathcal{F}}(\omega) = \frac{\omega^2}{2\pi} \int_C ds \, \mathrm{e}^{-\mathrm{i}\omega s} \, K_0(\mathrm{i}ms)$$

$$= \frac{\omega^2}{2} \, \mathrm{Im} \int_0^\infty ds \, \mathrm{e}^{-\mathrm{i}\omega s} \, H_0^{(2)}(ms) \; , \tag{B.4}$$

where we have first integrated by parts twice, as allowed by the large s behaviour of the integrand, then deformed C to the real s axis, as allowed by the merely logarithmic singularity of the integrand at $s = 0$, and finally used the Bessel function analytic continuation formulas [48]. The integral in (B.4) was encountered in [19] in the context of a non-derivative detector, and from equations (5.11) and (5.14) therein we have

$$\dot{\mathcal{F}}(\omega) = \frac{\omega^2}{\sqrt{\omega^2 - m^2}}\,\Theta(-\omega - m)\ , \tag{B.5}$$

which is the result (3.4a) used in the main text.

B.2.2 $\widetilde{\mathcal{M}}$

In $\widetilde{\mathcal{M}}$, we find from (3.3) that the integrand in (2.17) contains the additional piece

$$\Delta\mathcal{A}(\tau, \tau'') = -\frac{\eta}{2\pi}\frac{d^2}{d\tau'^2}K_0\left[m\sqrt{4d^2 - (\tau' - \tau'' - \mathrm{i}\epsilon)^2}\right]\ , \tag{B.6}$$

where the branch of the square root is as explained in the main text. The additional piece in the transition rate (2.17) is hence

$$\begin{aligned}
\Delta\dot{\mathcal{F}}(\omega) &= -\frac{\eta}{2\pi}\int_{-\infty}^{\infty}ds\,\mathrm{e}^{-\mathrm{i}\omega s}\frac{d^2}{ds^2}K_0\left[m\sqrt{4d^2 - (s - \mathrm{i}\epsilon)^2}\right] \\
&= \frac{\eta\omega^2}{2\pi}\int_{-\infty}^{\infty}ds\,\mathrm{e}^{-\mathrm{i}\omega s}\,K_0\left[m\sqrt{4d^2 - (s - \mathrm{i}\epsilon)^2}\right] \\
&= \frac{\eta\omega^2}{\pi}\,\mathrm{Re}\int_{0}^{\infty}ds\,\mathrm{e}^{-\mathrm{i}\omega s}\,K_0\left[m\sqrt{4d^2 - (s - \mathrm{i}\epsilon)^2}\right]\ , \tag{B.7}
\end{aligned}$$

again assuming $\omega \neq -m$ and integrating by parts twice. The integral in (B.7) was encountered in [19], and from equations (5.15) and (5.25) therein we have

$$\Delta\dot{\mathcal{F}}(\omega) = \frac{\eta\omega^2\cos\!\left(2d\sqrt{\omega^2 - m^2}\right)}{\sqrt{\omega^2 - m^2}}\,\Theta(-\omega - m)\ , \tag{B.8}$$

which leads to the result (3.4b) in the main text.

C Asymptotic past and future transition rate in the receding mirror spacetime

In this appendix we find the asymptotic past and future forms (4.9) and (4.12) of the transition rate of an inertial detector in the receding mirror spacetime of Section 4.

C.1 Static in the distant past

We wish to extract the asymptotic behaviour of (4.8) as $\tau \to -\infty$ and as $\tau \to \infty$.

C.1.1 $\tau \to -\infty$

Consider (4.8b). Using (4.5) and letting $h \doteq \left(1 + e^{\kappa(d-\tau)}\right)^{-1}$, we have

$$\dot{\mathcal{F}}_0(\omega,\tau) = -\omega\Theta(-\omega) + \frac{1}{2\pi}\int_0^\infty ds\,\cos(\omega s)\left(\frac{1}{X} + \frac{1}{s^2}\right)\,, \tag{C.1}$$

where

$$X = -\frac{[1 - h(1 - e^{-\kappa s})]\left\{\kappa s + \ln[1 - h(1 - e^{-\kappa s})]\right\}^2}{\kappa^2(1-h)^2}\,. \tag{C.2}$$

The limit $\tau \to -\infty$ is now the limit $h \to 0_+$.

Following the technique used in subsection 5.3 of [13], we make in the integrand of (C.1) the re-arrangement

$$\frac{1}{X} + \frac{1}{s^2} = \frac{-X - s^2}{s^4}\left(1 + \frac{-X - s^2}{s^2}\right)^{-1}\,. \tag{C.3}$$

Taylor expanding the numerator of (C.2) to quartic order in $h(1 - e^{-\kappa s})$ shows that the second factor in (C.3) is of the form $1 + O(h)$, uniformly in s, and yields for the first factor in (C.3) an estimate that can be applied under the integral over s and whose leading term is proportional to h. We hence have

$$\dot{\mathcal{F}}_0(\omega,\tau) = -\omega\Theta(-\omega) + O(h)\,. \tag{C.4}$$

Consider then (4.8c). Proceeding similarly, we find

$$\dot{\mathcal{F}}_1(\omega,\tau) = \frac{1}{4\pi d} + \frac{|\omega|}{2\pi}\left[\cos(2d\omega)\,\text{si}(2d|\omega|) - \sin(2d|\omega|)\,\text{Ci}(2d|\omega|)\right] + O(h)\,, \tag{C.5}$$

where si and Ci are the sine and cosine integrals in the notation of [48].

Consider finally (4.8d). Integrating by parts once reduces the integral to a form that can be evaluated exactly in terms of the sine and cosine integrals [48], with the result

$$\dot{\mathcal{F}}_2(\omega,\tau) = \frac{1-h}{2\pi}\left\{-\frac{1}{B} + |\omega|\left[\sin(B|\omega|)\,\text{Ci}(B|\omega|) - \cos(B\omega)\,\text{si}(B|\omega|)\right]\right.$$

$$\left. + 2\pi\omega\cos(B\omega)\Theta(-\omega)\right\}\,, \tag{C.6}$$

where $B \doteq 2d - \kappa^{-1} \ln(1 - h)$. A small h expansion in (C.6) gives

$$\dot{\mathcal{F}}_2(\omega, \tau) = -\frac{1}{4\pi d} + \frac{|\omega|}{2\pi} \left[\sin(2d|\omega|) \operatorname{Ci}(2d|\omega|) - \cos(2d\omega) \operatorname{si}(2d|\omega|)\right]$$

$$+ \omega \cos(B\omega)\Theta(-\omega) + O(h) . \tag{C.7}$$

Combining (C.4), (C.5) and (C.7), we have

$$\dot{\mathcal{F}}(\omega, \tau) = -\omega \left[1 - \cos(2d\omega)\right] \Theta(-\omega) + O(e^{\kappa\tau}) \quad \text{as } \tau \to -\infty . \tag{C.8}$$

C.1.2 $\quad \tau \to \infty$

Consider (4.8b). Letting $f \doteq 1/(1 + e^{\kappa(\tau-d)})$, and adding and subtracting $\kappa^2 \cos(\omega s)[8\pi \sinh^2(\kappa s/2)]^{-1}$ in the integrand, we obtain

$$\dot{\mathcal{F}}_0(\omega, \tau) = -\omega\Theta(-\omega) + \frac{1}{2\pi} \int_0^\infty ds \, \cos(\omega s) \left(\frac{1}{s^2} - \frac{\kappa^2}{4 \sinh^2(\kappa s/2)}\right)$$

$$+ \frac{\kappa^2}{2\pi} \int_0^\infty ds \, \cos(\omega s) \left(\frac{1}{4 \sinh^2(\kappa s/2)} - \frac{f^2 \, e^{\kappa s}}{[1 + f(e^{\kappa s} - 1)]\{\ln[1 + f(e^{\kappa s} - 1)]\}^2}\right) . \tag{C.9}$$

In the last term in (C.9), the integrand goes to zero pointwise as $f \to 0$, and a monotone convergence argument shows that the integral vanishes as $f \to 0$. The second term plus half of the first term is equal to half of the transition rate encountered in subsection 3.2 (with $a \to \kappa$) and evaluated to (3.10). We hence have

$$\dot{\mathcal{F}}_0(\omega, \tau) = -\frac{\omega}{2}\Theta(-\omega) + \frac{\omega}{2 \left(e^{2\pi\omega/\kappa} - 1\right)} + o(1) \quad \text{as } f \to 0 . \tag{C.10}$$

In (4.8c), a straightforward monotone convergence argument gives $\dot{\mathcal{F}}_1(\omega, \tau) = o(1)$. In (4.8d), (C.6) gives $\dot{\mathcal{F}}_2(\omega, \tau) = O(f)$.

Combining, we have

$$\dot{\mathcal{F}}(\omega, \tau) = -\frac{\omega}{2}\Theta(-\omega) + \frac{\omega}{2 \left(e^{2\pi\omega/\kappa} - 1\right)} + o(1) \quad \text{as } \tau \to \infty . \tag{C.11}$$

C.2 Travelling towards the mirror in the distant past

We wish to extract the asmptotic behaviour of (4.11) as $\tau \to -\infty$ and as $\tau \to \infty$.

C.2.1 $\quad \tau \to -\infty$

For (4.11b), proceeding as in (C.1)–(C.4) gives

$$\dot{\mathcal{F}}_0(\omega, \tau) = -\omega\Theta(-\omega) + O(e^{e^{\lambda\kappa\tau}}) . \tag{C.12}$$

For (4.11c), we have

$$\dot{\mathcal{F}}_1(\omega, \tau) = \frac{1}{2\pi} \int_0^\infty \frac{\cos(\omega s)\, ds}{\left(1 + g e^{-\kappa s e^\lambda}\right) \left[s e^\lambda - 2\tau \sinh \lambda + \kappa^{-1} \ln\left(1 + g e^{-\kappa s e^\lambda}\right)\right]^2} , \qquad \text{(C.13)}$$

where $g = e^{\kappa \tau e^\lambda}$. When $\tau < 0$, we may bound the absolute value of $\dot{\mathcal{F}}_1(\omega, \tau)$ by the replacements $\cos(\omega s) \to 1$ and $g \to 0$ in (C.13), and evaluating the integral that ensues gives $\dot{\mathcal{F}}_1(\omega, \tau) = O(\tau^{-1})$.

For (4.11d), we proceed as with (C.6), obtaining the exact result

$$\dot{\mathcal{F}}_2(\omega, \tau) = \frac{(1 - h)\, e^{2\lambda}}{2\pi} \left\{ -\frac{1}{C} + |\omega| \left[\sin(C|\omega|) \operatorname{Ci}(C|\omega|) - \cos(C\omega) \operatorname{si}(C|\omega|)\right] \right.$$

$$\left. + 2\pi\omega \cos(C\omega)\Theta(-\omega) \right\} , \qquad \text{(C.14)}$$

where $h = g/(1 + g)$ and $C \doteq -(e^{2\lambda} - 1)\tau - \kappa^{-1}e^\lambda \ln(1 - h)$. As $\tau \to -\infty$, we have $C \to \infty$, and using formulas (6.2.17) and (6.12.3) in [48] gives

$$\dot{\mathcal{F}}_2(\omega, \tau) = e^{2\lambda}\, \omega \cos(2\tau \sinh \lambda\, e^\lambda \omega)\Theta(-\omega) + O(\tau^{-3}) . \qquad \text{(C.15)}$$

Combining, we have

$$\dot{\mathcal{F}}(\omega, \tau) = -\omega \left[1 - e^{2\lambda} \cos(2\tau \sinh \lambda\, e^\lambda \omega)\right] \Theta(-\omega) + O(\tau^{-1}) . \qquad \text{(C.16)}$$

C.2.2 $\quad \tau \to \infty$

For (4.11b), proceeding as in (C.9) gives

$$\dot{\mathcal{F}}_0(\omega, \tau) = -\frac{\omega}{2}\Theta(-\omega) + \frac{\omega}{2\left(e^{2\pi e^{-\lambda}\omega/\kappa} - 1\right)} + o(1) \quad \text{as } \tau \to \infty. \qquad \text{(C.17)}$$

For (4.11c), using (C.13) and substituting $s = \tau + r$ gives

$$\dot{\mathcal{F}}_1(\omega, \tau) = \frac{\kappa^2}{2\pi} \int_{-\tau}^\infty \frac{\cos[\omega(\tau + r)]\, ds}{\left(1 + e^{-\kappa r e^\lambda}\right) \left[\kappa \tau e^{-\lambda} + \ln\left(1 + e^{\kappa r e^\lambda}\right)\right]^2} . \qquad \text{(C.18)}$$

We may assume $\tau > 0$. To bound the absolute value of (C.18), we make in the integrand the replacement $\cos[\omega(\tau + r)] \to 1$ and extend the integration to be over the full real axis in r. Elementary estimates then show that the contribution from $-\infty < r < 0$ is $O(\tau^{-2})$ and the contribution from from $0 < r < \infty$ is $O(\tau^{-1})$. Hence $\dot{\mathcal{F}}_1(\omega, \tau) = O(\tau^{-1})$.

For (4.11d), (C.14) gives $\dot{\mathcal{F}}_2(\omega, \tau) = O\left(e^{-e^\lambda \kappa \tau}\right)$.

Combining, we have

$$\dot{\mathcal{F}}(\omega, \tau) = -\frac{\omega}{2}\Theta(-\omega) + \frac{\omega}{2\left(e^{2\pi e^{-\lambda}\omega/\kappa} - 1\right)} + o(1) \quad \text{as } \tau \to \infty. \qquad \text{(C.19)}$$

37

D Near-infinity and near-singularity transition rates in the $(1 + 1)$-dimensional Schwarzschild spacetime

In this appendix we verify the near-infinity and near-singularity transition rate formulas (5.17) and (5.18) for the inertial detector in the $(1 + 1)$-dimensional Schwarzschild spacetime.

D.1 Near-infinity transition rate

We consider the $E \geq 1$ trajectories (5.13) and (5.14) in Quadrant I. We wish to find the transition rate in the early time limit, assuming that the detector is switched on in the asymptotic past.

Using (2.16) and (5.10), we find

$$
\dot{\mathcal{F}}_B(\omega, \tau) = -\omega\Theta(-\omega) + 2\int_0^\infty ds \cos(\omega s) \left(\mathcal{A}_u(\tau, \tau - s) + \mathcal{A}_v(\tau, \tau - s) + \frac{1}{2\pi s^2} \right) ,
$$
$$(D.1a)$$

$$
\dot{\mathcal{F}}_H(\omega, \tau) = -\omega\Theta(-\omega) + 2\int_0^\infty ds \cos(\omega s) \left(\mathcal{A}_{\bar{u}}(\tau, \tau - s) + \mathcal{A}_{\bar{v}}(\tau, \tau - s) + \frac{1}{2\pi s^2} \right) ,
$$
$$(D.1b)$$

$$
\dot{\mathcal{F}}_U(\omega, \tau) = -\omega\Theta(-\omega) + 2\int_0^\infty ds \cos(\omega s) \left(\mathcal{A}_{\bar{u}}(\tau, \tau - s) + \mathcal{A}_v(\tau, \tau - s) + \frac{1}{2\pi s^2} \right) ,
$$
$$(D.1c)$$

where

$$
\mathcal{A}_u(\tau, \tau') = -\frac{\dot{u}(\tau)\dot{u}(\tau')}{4\pi[u(\tau) - u(\tau')]^2} , \tag{D.2a}
$$

$$
\mathcal{A}_v(\tau, \tau') = -\frac{\dot{v}(\tau)\dot{v}(\tau')}{4\pi[v(\tau) - v(\tau')]^2} , \tag{D.2b}
$$

$$
\mathcal{A}_{\bar{u}}(\tau, \tau') = -\frac{\dot{\bar{u}}(\tau)\dot{\bar{u}}(\tau')}{4\pi[\bar{u}(\tau) - \bar{u}(\tau')]^2} , \tag{D.2c}
$$

$$
\mathcal{A}_{\bar{v}}(\tau, \tau') = -\frac{\dot{\bar{v}}(\tau)\dot{\bar{v}}(\tau')}{4\pi[\bar{v}(\tau) - \bar{v}(\tau')]^2} . \tag{D.2d}
$$

Using (5.13) and (5.14), it is straightforward to verify that as $\tau \to -\infty$ with fixed

positive s, we have

$$\mathcal{A}_u(\tau, \tau - s) \to -\frac{1}{4\pi s^2} \ , \tag{D.3a}$$

$$\mathcal{A}_v(\tau, \tau - s) \to -\frac{1}{4\pi s^2} \ , \tag{D.3b}$$

$$\mathcal{A}_{\bar{u}}(\tau, \tau - s) \to -\frac{e^{2\lambda}}{4\pi(8M)^2 \sinh^2\big(e^\lambda s/(8M)\big)} \ , \tag{D.3c}$$

$$\mathcal{A}_{\bar{v}}(\tau, \tau - s) \to -\frac{e^{-2\lambda}}{4\pi(8M)^2 \sinh^2\big(e^{-\lambda}s/(8M)\big)} \ , \tag{D.3d}$$

where $\lambda = \operatorname{arctanh}\big(\sqrt{1 - E^{-2}}\,\big)$. Taking the $\tau \to -\infty$ limit under the integrals in (D.1), justified by the monotone convergence argument given below, and proceeding as in subsection 3.2, leads to the formulas (5.17) in the main text.

What remains is to provide the monotone convergence argument. Let q stand for either $\dot{u}$ or $\dot{v}$, and note from (5.4) and (5.12) that

$$\dot{r} = -\sqrt{E^2 - 1 + 2M/r} \ , \tag{D.4a}$$

$$q = \frac{1}{E + \eta\sqrt{E^2 - 1 + 2M/r}} \ , \tag{D.4b}$$

$$\dot{q} = -\frac{\eta M}{r^2 \left(E + \eta\sqrt{E^2 - 1 + 2M/r} \right)^2} \ , \tag{D.4c}$$

where $\eta = 1$ for $q = \dot{v}$ and $\eta = -1$ for $q = \dot{u}$. The expressions

$$\frac{\int_{\tau-s}^{\tau} q(\tau')\,d\tau'}{\sqrt{q(\tau)q(\tau - s)}} \ , \tag{D.5a}$$

$$\frac{\sinh\left(\frac{1}{8M}\int_{\tau-s}^{\tau} q(\tau')\,d\tau'\right)}{\sqrt{q(\tau)q(\tau - s)}} \ , \tag{D.5b}$$

are hence well defined for all $s > 0$ when τ is sufficiently large and negative. For monotone convergence, it suffices to show that each of the expressions in (D.5) is monotone in τ for all $s > 0$ when τ is sufficiently large and negative. Differentiating (D.5) with respect to τ, it suffices to show that each of the expressions

$$\int_{\tau-s}^{\tau} q(\tau')\,d\tau' - 2[q(\tau) - q(\tau - s)] \left(\frac{\dot{q}(\tau)}{q(\tau)} + \frac{\dot{q}(\tau - s)}{q(\tau - s)} \right)^{-1} \ , \tag{D.6a}$$

$$\tanh\left(\frac{1}{8M}\int_{\tau-s}^{\tau} q(\tau')\,d\tau'\right) - \frac{1}{4M}[q(\tau) - q(\tau - s)] \left(\frac{\dot{q}(\tau)}{q(\tau)} + \frac{\dot{q}(\tau - s)}{q(\tau - s)} \right)^{-1} \ , \tag{D.6b}$$

has a fixed sign for all $s > 0$ when τ is sufficiently large and negative. Introducing in (D.6) a new integration variable by $p' = \sqrt{E^2 - 1 + 2M/r(\tau')}$, we see that it suffices to show that each of the functions

$$f_1(p) = \frac{1}{2} \int_p^{p_f} \frac{dp'}{(E + \eta p')[p'^2 - E^2 + 1]^2}$$

$$- \frac{p_f - p}{(E + \eta p)[p_f^2 - E^2 + 1]^2 + (E + \eta p_f)[p^2 - E^2 + 1]^2} \ , \tag{D.7a}$$

$$f_2(p) = \tanh\left(\frac{1}{2} \int_p^{p_f} \frac{dp'}{(E + \eta p')[p'^2 - E^2 + 1]^2} \right)$$

$$- \frac{p_f - p}{(E + \eta p)[p_f^2 - E^2 + 1]^2 + (E + \eta p_f)[p^2 - E^2 + 1]^2} \ , \tag{D.7b}$$

defined on the domain $\sqrt{E^2 - 1} < p < p_f$, where $p_f \in \left(\sqrt{E^2 - 1}, E \right)$ is a parameter, has a fixed sign when p_f is sufficiently close to $\sqrt{E^2 - 1}$.

Consider f_1. f_1' is a rational function whose sign can be analysed by elementary methods, with the outcome that f_1' is negative when p_f is sufficiently close to $\sqrt{E^2 - 1}$. Hence f_1 is positive when p_f is sufficiently close to $\sqrt{E^2 - 1}$.

Consider then f_2. When p_f is sufficiently close to $\sqrt{E^2 - 1}$, an elementary analysis shows that the second term in (D.7b) is negative and strictly increasing, and there is a $p_1 \in \left(\sqrt{E^2 - 1}, p_f \right)$ such that this term takes the value -1 at $p = p_1$. With p_f this close to $\sqrt{E^2 - 1}$, it follows that f_2 is negative for $p \leq p_1$, whereas for $p_1 < p < p_f$ f_2 has the same sign as

$$f_3(p) = \frac{1}{2} \int_p^{p_f} \frac{dp'}{(E + \eta p')[p'^2 - E^2 + 1]^2}$$

$$- \operatorname{arctanh}\left(\frac{p_f - p}{(E + \eta p)[p_f^2 - E^2 + 1]^2 + (E + \eta p_f)[p^2 - E^2 + 1]^2} \right) . \tag{D.8}$$

f_3 can be analysed by the same methods as f_1, with the outcome that f_3 is negative when p_f is sufficiently close to $\sqrt{E^2 - 1}$. Collecting, we see that f_2 is negative when p_f is sufficiently close to $\sqrt{E^2 - 1}$.

This completes the monotone convergence argument.

D.2 Near-singularity transition rate

We consider the trajectories (5.13), (5.14), (5.15) and (5.16), with $E \geq 0$, and with the field in the HHI and Unruh vacua. The switch-off moment τ is assumed to be in Quadrant II. The switch-on-moment τ_0 either is finite and in a region of the spacetime where the vacuum is regular, or for $E \geq 1$ may alternatively be pushed to the asymptotic past.

Let τ_{sing} be the value of τ at the black hole singularity, and let τ_1 be a constant such that the detector is somewhere in Quadrant II at proper time τ_1. In the limit $\tau \to \tau_{\text{sing}}$ with everything else fixed, we have

$$\dot{\mathcal{F}}_H(\omega, \tau) = G_{\bar{u}}(\omega, \tau, \tau_1) + G_{\bar{v}}(\omega, \tau, \tau_1) + O(1) , \tag{D.9a}$$

$$\dot{\mathcal{F}}_U(\omega, \tau, \tau_1) = G_{\bar{u}}(\omega, \tau, \tau_1) + G_v(\omega, \tau, \tau_1) + O(1) , \tag{D.9b}$$

where

$$G_v(\omega, \tau, \tau_1) = 2 \int_{\tau_1}^{\tau} d\tau' \cos[\omega(\tau - \tau')] \left(\mathcal{A}_v(\tau, \tau') + \frac{1}{4\pi(\tau - \tau')^2} \right) , \tag{D.10a}$$

$$G_{\bar{v}}(\omega, \tau, \tau_1) = 2 \int_{\tau_1}^{\tau} d\tau' \cos[\omega(\tau - \tau')] \left(\mathcal{A}_{\bar{v}}(\tau, \tau') + \frac{1}{4\pi(\tau - \tau')^2} \right) , \tag{D.10b}$$

$$G_{\bar{u}}(\omega, \tau, \tau_1) = 2 \int_{\tau_1}^{\tau} d\tau' \cos[\omega(\tau - \tau')] \left(\mathcal{A}_{\bar{u}}(\tau, \tau') + \frac{1}{4\pi(\tau - \tau')^2} \right) , \tag{D.10c}$$

and $\mathcal{A}_v$, $\mathcal{A}_{\bar{v}}$ and $\mathcal{A}_{\bar{u}}$ are given in (D.2).

Consider first $G_v(\omega, \tau, \tau_1)$, and assume $\tau_1 < \tau < \tau_{\text{sing}}$. Working in the coordinates (v, r), well defined in Quadrant II, the equations for the trajectory read

$$\dot{r} = -\sqrt{E^2 - 1 + 2M/r} , \tag{D.11a}$$

$$\dot{v} = \frac{1}{E + \sqrt{E^2 - 1 + 2M/r}} , \tag{D.11b}$$

from which it follows that

$$\ddot{v} = -\frac{M}{r^2 \left(E + \sqrt{E^2 - 1 + 2M/r} \right)^2} . \tag{D.12}$$

From (D.2b) and (D.10a) we hence have

$$G_v(\omega, \tau, \tau_1) = \frac{1}{2\pi} \lim_{\tau' \to \tau} \left[\cos[\omega(\tau - \tau')] \left(-\frac{\dot{v}(\tau)}{v(\tau) - v(\tau')} + \frac{1}{\tau - \tau'} \right) \right] + O(1)$$

$$= \frac{1}{16\pi M} \left[\left(\frac{2M}{r(\tau)} \right)^{3/2} - E \left(\frac{2M}{r(\tau)} \right) + \frac{1 + E^2}{2} \left(\frac{2M}{r(\tau)} \right)^{1/2} \right] + O(1) , \tag{D.13}$$

where we have first integrated by parts, observing that the new integral term is $O(1)$ by virtue of near-singularity estimates that ensue from (D.11) and (D.12), and then evaluated the limit using (D.11) and (D.12).

For $G_{\bar{v}}(\omega, \tau, \tau_1)$ we may proceed similarly, using $\bar{v} = 4M \exp[v/(4M)]$. The differences from $G_v(\omega, \tau, \tau_1)$ turn out to be $O(1)$, so that

$$G_{\bar{v}}(\omega, \tau, \tau_1) = \frac{1}{16\pi M} \left[\left(\frac{2M}{r(\tau)} \right)^{3/2} - E \left(\frac{2M}{r(\tau)} \right) + \frac{1 + E^2}{2} \left(\frac{2M}{r(\tau)} \right)^{1/2} \right] + O(1) . \tag{D.14}$$

For $G_{\bar{u}}(\omega, \tau, \tau_1)$ the analysis is as for $G_{\bar{v}}(\omega, \tau, \tau_1)$ but with $E \to -E$, with the result

$$G_{\bar{u}}(\omega, \tau, \tau_1) = \frac{1}{16\pi M} \left[\left(\frac{2M}{r(\tau)} \right)^{3/2} + E \left(\frac{2M}{r(\tau)} \right) + \frac{1 + E^2}{2} \left(\frac{2M}{r(\tau)} \right)^{1/2} \right] + O(1) \, . \quad (D.15)$$

Combining (D.9), (D.13), (D.14) and (D.15) yields (5.18).

References

[1] N. D. Birrell and P. C. W. Davies, *Quantum Fields in Curved Space* (Cambridge University Press, 1982).

[2] R. M. Wald, *Quantum field theory in curved spacetime and black hole thermodynamics* (University of Chicago Press, Chicago, 1994).

[3] W. G. Unruh, "Notes on black hole evaporation," Phys. Rev. D **14**, 870 (1976).

[4] S. W. Hawking, "Particle creation by black holes," Commun. Math. Phys. **43**, 199 (1975) [Erratum-ibid. **46**, 206 (1976)].

[5] G. W. Gibbons and S. W. Hawking, "Cosmological event horizons, thermodynamics, and particle creation," Phys. Rev. D **15**, 2738 (1977).

[6] B. S. DeWitt, "Quantum gravity: the new synthesis", in *General Relativity: an Einstein centenary survey*, edited by S. W. Hawking and W. Israel (Cambridge University Press, Cambridge, 1979) 680.

[7] S. Takagi, "Vacuum noise and stress induced by uniform acceleration: Hawking-Unruh effect in Rindler manifold of arbitrary dimension," Prog. Theor. Phys. Suppl. **88**, 1 (1986).

[8] L. C. B. Crispino, A. Higuchi and G. E. A. Matsas, "The Unruh effect and its applications," Rev. Mod. Phys. **80**, 787 (2008) [arXiv:0710.5373].

[9] P. C. W. Davies and A. C. Ottewill, "Detection of negative energy: 4-dimensional examples," Phys. Rev. D **65**, 104014 (2002) [arXiv:gr-qc/0203003].

[10] S. Schlicht, "Considerations on the Unruh effect: Causality and regularization," Class. Quant. Grav. **21**, 4647 (2004) [arXiv:gr-qc/0306022].

[11] P. Langlois, "Causal particle detectors and topology," Annals Phys. **321**, 2027 (2006) [arXiv:gr-qc/0510049].

[12] P. Langlois, "Imprints of spacetime topology in the Hawking-Unruh effect", PhD Thesis, University of Nottingham (2005) [arXiv:gr-qc/0510127].

[13] J. Louko and A. Satz, "How often does the Unruh-DeWitt detector click? Regularisation by a spatial profile," Class. Quant. Grav. **23**, 6321 (2006) [arXiv:gr-qc/0606067].

[14] A. Satz, "Then again, how often does the Unruh-DeWitt detector click if we switch it carefully?," Class. Quant. Grav. **24**, 1719 (2007) [arXiv:gr-qc/0611067].

[15] J. Louko and A. Satz, "Transition rate of the Unruh-DeWitt detector in curved spacetime", Class. Quant. Grav. **25**, 055012 (2008) [arXiv:0710.5671 [gr-qc]].

[16] L. Hodgkinson and J. Louko, "How often does the Unruh-DeWitt detector click beyond four dimensions?", *J. Math. Phys.* **53**, 082301 (2012) [arXiv:1109.4377v3 [gr-qc]].

[17] L. Hodgkinson and J. Louko, "Static, stationary and inertial Unruh-DeWitt detectors on the BTZ black hole," Phys. Rev. D **86**, 064031 (2012) [arXiv:1206.2055 [gr-qc]].

[18] L. C. Barbado and M. Visser, "Unruh-DeWitt detector event rate for trajectories with time-dependent acceleration," Phys. Rev. D **86**, 084011 (2012) [arXiv:1207.5525 [gr-qc]].

[19] L. Hodgkinson, "Particle detectors in curved spacetime quantum field theory," PhD Thesis, University of Nottingham (2013) [arXiv:1309.7281v2 [gr-qc]].

[20] L. Hodgkinson, J. Louko and A. C. Ottewill, "Static detectors and circular-geodesic detectors on the Schwarzschild black hole," Phys. Rev. D **89**, 104002 (2014) [arXiv:1401.2667 [gr-qc]].

[21] K. K. Ng, L. Hodgkinson, J. Louko, R. B. Mann and E. Martín-Martínez, "Unruh-DeWitt detector response along static and circular-geodesic trajectories for Schwarzschild-AdS black holes," Phys. Rev. D **90**, 064003 (2014) [arXiv:1406.2688 [quant-ph]].

[22] A. Raval, B. L. Hu and J. Anglin, "Stochastic theory of accelerated detectors in a quantum field," Phys. Rev. D **53**, 7003 (1996) [arXiv:gr-qc/9510002].

[23] S. -Y. Lin and B. L. Hu, "Backreaction and the Unruh effect: New insights from exact solutions of uniformly accelerated detectors," Phys. Rev. D **76**, 064008 (2007) [gr-qc/0611062].

[24] D. C. M. Ostapchuk, S. -Y. Lin, R. B. Mann and B. L. Hu, "Entanglement Dynamics between Inertial and Non-uniformly Accelerated Detectors," JHEP **1207**, 072 (2012) [arXiv:1108.3377 [gr-qc]].

[25] E. G. Brown, E. Martín-Martínez, N. C. Menicucci and R. B. Mann, "Detectors for probing relativistic quantum physics beyond perturbation theory," Phys. Rev. D **87**, 084062 (2013) [arXiv:1212.1973 [quant-ph]].

[26] D. E. Bruschi, A. R. Lee and I. Fuentes, "Time evolution techniques for detectors in relativistic quantum information," J. Phys. A **46**, 165303 (2013) [arXiv:1212.2110 [quant-ph]].

[27] B. L. Hu, S. -Y. Lin and J. Louko, "Relativistic quantum information in detectors-field interactions," Class. Quant. Grav. **29**, 224005 (2012) [arXiv:1205.1328 [quant-ph]].

[28] P. C. W. Davies and S. A. Fulling, "Radiation from a moving mirror in two-dimensional space-time conformal anomaly," Proc. Roy. Soc. Lond. A **348**, 393 (1976).

[29] P. C. W. Davies and S. A. Fulling, "Radiation from moving mirrors and from black holes," Proc. Roy. Soc. Lond. A **356**, 237 (1977).

[30] Y. Décanini and A. Folacci, "Hadamard renormalization of the stress-energy tensor for a quantized scalar field in a general spacetime of arbitrary dimension," Phys. Rev. D **78**, 044025 (2008) [arXiv:gr-qc/0512118].

[31] S. A. Fulling and S. N. M. Ruijsenaars, "Temperature, periodicity and horizons," Phys. Rept. **152**, 135 (1987).

[32] B. S. Kay, "Application of linear hyperbolic PDE to linear quantum fields in curved space-times: Especially black holes, time machines and a new semilocal vacuum concept," Journées Équations aux dérivées partielles, Nantes, 5 au 9 juin 2000, GDR 1151 (CNRS), IX-1 [arXiv:gr-qc/0103056].

[33] D. J. Raine, D. W. Sciama and P. G. Grove, "Does an accelerated oscillator radiate?" Proc. Roy. Soc. A **435**, 205 (1991).

[34] Q. Wang and W. G. Unruh, "Motion of a mirror under infinitely fluctuating quantum vacuum stress," Phys. Rev. D **89**, 085009 (2014) [arXiv:1312.4591 [gr-qc]].

[35] R. Kubo, "Statistical mechanical theory of irreversible processes. 1. General theory and simple applications in magnetic and conduction problems," J. Phys. Soc. Jap. **12**, 570 (1957).

[36] P. C. Martin and J. S. Schwinger, "Theory of many particle systems. 1.," Phys. Rev. **115**, 1342 (1959).

[37] E. Martín-Martínez and J. Louko, "Particle detectors and the zero mode of a quantum field," Phys. Rev. D **90**, 024015 (2014) [arXiv:1404.5621 [quant-ph]].

[38] P. Anderson, R. Balbinot, A. Fabbri and R. Parentani, "Gray-body factor and infrared divergences in BEC acoustic black holes," arXiv:1404.3224 [gr-qc].

[39] S. L. Braunstein, "Black hole entropy as entropy of entanglement, or it's curtains for the equivalence principle," arXiv:0907.1190v1 [quant-ph]; S. L. Braunstein, S. Pirandola and K. Życzkowski, "Better Late than Never: Information Retrieval from Black Holes," Phys. Rev. Lett. **110**, 101301 (2013) [arXiv:0907.1190v3 [quant-ph]].

[40] S. D. Mathur, "The information paradox: a pedagogical introduction," Class. Quant. Grav. **26**, 224001 (2009) [arXiv:0909.1038 [hep-th]].

[41] A. Almheiri, D. Marolf, J. Polchinski and J. Sully, "Black Holes: Complementarity or Firewalls?," JHEP **1302**, 062 (2013) [arXiv:1207.3123 [hep-th]].

[42] M. Hotta, J. Matsumoto and K. Funo, "Black hole firewalls require huge energy of measurement," Phys. Rev. D **89**, 124023 (2014) [arXiv:1306.5057 [quant-ph]].

[43] A. Almheiri and J. Sully, "An Uneventful Horizon in Two Dimensions," JHEP **1402**, 108 (2014) [arXiv:1307.8149 [hep-th]].

[44] C. J. Fewster, "A general worldline quantum inequality," Class. Quant. Grav. **17**, 1897 (2000) [arXiv:gr-qc/9910060].

[45] W. Junker and E. Schrohe, "Adiabatic vacuum states on general space-time manifolds: Definition, construction, and physical properties," Ann. Henri Poincaré **3**, 1113 (2002) [arXiv:math-ph/0109010].

[46] L. Hörmander, *The Analysis of Linear Partial Differential Operators I (Distribution Theory and Fourier Analysis)*, 2nd Edition (Springer, Berlin, 1990), Theorem 8.2.4.

[47] L. Hörmander, "Fourier Integral Operators. I", Acta Mathematica **127**, 79 (1971), Theorem 2.5.11'. Reprinted in: J. Brüning and V. W. Guillemin (Editors), *Fourier Integral Operators* (Springer, Berlin, 1994).

[48] NIST Digital Library of Mathematical Functions. `http://dlmf.nist.gov/`, Release 1.0.6 of 2013-05-06.

[49] I. S. Gradshteyn and I. M. Ryzhik, *Table of Integrals, Series, and Products*, 7th edition (Academic Press, New York, 2007).

[50] R. D. Carlitz and R. S. Willey, "Reflections on moving mirrors," Phys. Rev. D **36**, 2327 (1987).

[51] M. R. R. Good, P. R. Anderson and C. R. Evans, "Time dependence of particle creation from accelerating mirrors," Phys. Rev. D **88**, 025023 (2013) [arXiv:1303.6756 [gr-qc]].

[52] C. W. Misner, K. S. Thorne and J. A. Wheeler, *Gravitation* (Freeman, San Francisco, 1973).

[53] D. G. Boulware, "Quantum field theory in Schwarzschild and Rindler spaces," Phys. Rev. D **11**, 1404 (1975).

[54] J. B. Hartle and S. W. Hawking, "Path integral derivation of black hole radiance," Phys. Rev. D **13**, 2188 (1976).

[55] W. Israel, "Thermofield dynamics of black holes," Phys. Lett. A **57**, 107 (1976).

[56] C. Dappiaggi, V. Moretti and N. Pinamonti, "Rigorous construction and Hadamard property of the Unruh state in Schwarzschild spacetime," Adv. Theor. Math. Phys. **15**, 355 (2011) [arXiv:0907.1034 [gr-qc]].

[57] C. Barcelo, S. Liberati, S. Sonego and M. Visser, "Minimal conditions for the existence of a Hawking-like flux," Phys. Rev. D **83** (2011) 041501 [arXiv:1011.5593 [gr-qc]].

[58] L. C. Barbado, C. Barcelo and L. J. Garay, "Hawking radiation as perceived by different observers," Class. Quant. Grav. **28** (2011) 125021 [arXiv:1101.4382 [gr-qc]].

[59] L. C. Barbado, C. Barcelo and L. J. Garay, "Hawking radiation as perceived by different observers: An analytic expression for the effective-temperature function," Class. Quant. Grav. **29** (2012) 075013 [arXiv:1201.3820 [gr-qc]].

[60] M. Smerlak and S. Singh, "New perspectives on Hawking radiation," Phys. Rev. D **88**, 104023 (2013) [arXiv:1304.2858 [gr-qc]].

[61] C. J. Fewster, B. A. Juárez-Aubry and J. Louko, in preparation (2014).